AD-A261 199

WHOI-92-15

Woods Hole Oceanographic Institution

Biogenic Particle Fluxes at the 34°N 21°W and 48°N 21°W Stations, 1989-1990: Methods and Analytical Data Compilation

by

Susumu Honjo and Steven J. Manganini

March 1992

Technical Report

Funding was provided by the National Science Foundation through Grant No. OCE 88-14228.

WHOI-92-15

Biogenic Particle Fluxes at the 34^0N 21^0W and 48^0N 21^0W Stations, 1989-1990: Methods and Analytical Data Compilation

by

Susumu Honjo and Steven J. Manganini

Woods Hole Oceanographic Institution
Woods Hole, Massachusetts 02543

March 1992

Technical Report

Funding was provided by the National Science Foundation through Grant No. OCE 88-14228.

Approved for Distribution:

G. Michael Purdy
Department of Geology & Geophysics

BIOGENIC PARTICLE FLUXES AT THE 34°N 21°W AND 48°N 21°W STATIONS, 1989-1990: METHODS AND ANALYTICAL DATA COMPILATION

by

Susumu Honjo and Steven J. Manganini
Woods Hole Oceanographic Institution
Woods Hole, MA 02543 USA

March 1992

Data appearing in this Technical Report have been submitted to the United States National Oceanographic Data Center, 1825 Connecticut Avenue, Washington, DC 20235. These data are also available from the United States JGOFS Data Management Office, Woods Hole Oceanographic Institution, Woods Hole, MA 02540.

5 key words: bloom
North Atlantic Ocean
ocean interior
particle flux
terminal ratio

TABLE OF CONTENTS

Abstract 1

Introduction 2

Method 3

Deployment of Sediment Traps and Mooring Arrays 3

Location, depths and timing 3

Time-series sediment trap 3

Mooring array 4

Laboratory Analysis 5

Pre-analysis treatment of samples 5

Supernatant analysis 5

Water sieving 5

Total dry mass measurement 6

Sedimentary component analyses 6

Restoration of dissolved components to particulate flux 8

Initial Bottle Water Concentration 8

Water Column Concentration 8

Final Bottle Water Concentration 9

Dissolved Components 9

Total Components 9

Formulae 9

Flux Calculations 9

Sample Collecting Time 10

Actual Collecting Time 10

Normalized Collecting Time 10

Formulae 10

Results 11

Annual Particle Flux 11

Variability of Particle Fluxes by Period 12

Variability of Particle Fluxes by Depth 13

Fluxes of Sedimentary Components 13
Ratios of Critical Biogeochemical Elements 14
Acknowledgments 15
References 16
Explanation of Figures 18
Figures
Figure 1 Locations 20
Figure 2 Transect Profiles 21
Figure 3 Mooring Schematics 22
Figure 4 Total Mass Fluxes; Annual Variability 23
Figure 5 Component Fluxes; Annual Variability 24
Figure 6 Proportions of Component Fluxes; Annual Variability 25
Figure 7 C_{org}/C_{CaCo_3}, Variability in Space and Time 26
Figure 8 Ratio Betv/een Biogenic Elements in Episodes 27
Explanation of Tables 28

Tables

Logistics Tables 31
Table 1 Mooring Stations and Trap Depths 32
Table 2 Synchronized Open/Close Schedule 33
Table 3 Sediment Trap Specifications 34

Preparation Tables 35
Table 4 Initial Water: location and depths 36
Table 5 Nutrient Concentration in Initial Water
Table 5-a at 34°N 21°W 37
Table 5-b at 48°N 21°W 38
Table 6 "Times" to deliver "Normalized Times" 39

Summary Tables 40
Table 7 Flux Summary 41
Table 8 34°N: Fluxes and Proportions Sedimentary Components 42
Table 9 48°N: Fluxes and Proportions Sedimentary Components 43

Table 10 34°N: Ratios Between Biogeochemical Elements 44
Table 11 48°N: Ratios Between Biogeochemical Elements 45
Table 12 "Redfield Ratio" 46

Tables Giving Flux per Period 47

Table 13: 34°N

Table 13-1: 1 km

Table 13-1-a Size Fractions 48
Table 13-1-b Fluxes of Ca, C_{inorg}, C_{org} and N_{org} 49
Table 13-1-c Opal Fluxes 50
Table 13-1-d Phosphorus Fluxes 51
Table 13-1-e Ratios (Molar) of Critical Elements 52

Table 13-2: 2 km

Table 13-2-a Size Fractions 53
Table 13-2-b Fluxes of Ca, C_{inorg}, C_{org} and N_{org} 54
Table 13-2-c Opal Fluxes 55
Table 13-2-d Phosphorus Fluxes 56
Table 13-2-e Ratios (Molar) of Critical Elements 57

Table 13-3: 0.7 km above bottom

Table 13-3-a Size Fractions 58
Table 13-3-b Fluxes of Ca, C_{inorg}, C_{org} and N_{org} 59
Table 13-3-c Opal Fluxes 60
Table 13-3-d Phosphorus Fluxes 61
Table 13-3-e Ratios (Molar) of Critical Elements 62

Table 14: 48°N

Table 14-1: 1 km

Table 14-1-a Size Fractions 63
Table 14-1-b Fluxes of Ca, C_{inorg}, C_{org} and N_{org} 64
Table 14-1-c Opal Fluxes 65
Table 14-1-d Phosphorus Fluxes 66
Table 14-1-e Ratios (Molar) of Critical Elements 67

Table 14-2: 2 km

Table 14-2-a Size Fractions 68

Table 14-2-b Fluxes of Ca, C_{inorg}, C_{org} and N_{org} 69

Table 14-2-c Opal Fluxes 70

Table 14-2-d Phosphorus Fluxes 71

Table 14-2-e Ratios (Molar) of Critical Elements 72

Table 14-3: 0.7 km above bottom

Table 14-3-a Size Fractions 73

Table 14-3-b Fluxes of Ca, C_{inorg}, C_{org} and N_{org} 74

Table 14-3-c Opal Fluxes 75

Table 14-3-d Phosphorus Fluxes 76

Table 14-3-e Ratios (Molar) of Critical Elements 77

BIOGENIC PARTICLE FLUXES AT THE 34°N 21°W AND 48°N 21°W STATIONS, 1989-1990: METHODS AND ANALYTICAL DATA COMPILATION

by

Susumu Honjo and Steven J. Manganini
Woods Hole Oceanographic Institution
Woods Hole, MA 02543 USA

ABSTRACT

This technical report presents the results of analyses on opal, organic carbon, nitrogen and phosphorus content in each of 156 specimen samples collected from the moored sediment trap experiment that was a part of JGOFS North Atlantic Bloom Experiment. The analyzed samples represent a spatio-temporal matrix formed by 6 time-series sediment traps that provided 26 periods of uniform and synchronized periods of 14 days, except for one longer and one shorter period. Traps were deployed at 3 depths, 1 km, 2 km and 0.7 km above the bottom, and at 2 stations, 34°N 21°W and 48°N 21°W from April 4, 1989 to April 17, 1990, as shown in Tables 1 and 2. There was an 20-day hiatus in September/October 1989 for changeover of the trap moorings. Some samples were unusable because of the intrusion of fish.

Samples were separated into several aliquots by wet-splitting, then water sieved into larger-than- and smaller-than-1-mm sizes. The fluxes of biogeochemical elements and constituents were determined on these aliquots and size fractions for: carbonate by vacuum gasometric method; opal by selective leaching method; reactive phosphorus by high temperature oxidation hydrolysis method; and organic carbon and nitrogen by applying an elementary analyzer. The annual fluxes, fluxes during the bloom, pre- and post-bloom episodes were normalized to a 365-day calendar year (Table 6) and are summarized in Tables 7 to 12. Variability of particle fluxes by each period at the two stations in terms of size fractions, sedimentary constituents and elements are shown in Tables 13 and 14. The molar ratios between pairs of critical biogeochemical elements during each episode and annually, shown at various depths and stations, are included in Tables 10 through 14.

INTRODUCTION

Six automated time-series sediment traps were deployed at three bathypelagic layers along bottom-tethered, moored arrays in the North Atlantic at 34°N 21°W and 48°N 21°W for about a year from the spring of 1989 to the spring of 1990, with the North Atlantic Bloom Study Experiment (NABE) organized by JGOFS and supported by the National Science Foundation, USA. The 34°N station is in the North Atlantic Subtropical Zone while the 48°N station is in the North Atlantic Transition Zone (Bradshaw, 1959; Okada and McIntyre, 1979) representing different physical and biogeographic ocean areas. This trap experiment was characterized by synchronizing the open/close timing of all 6 traps that provided us with a time-space matrix in depth (1, 2 and 4.5 or 5 km) and latitude (1,256 km apart); these conditions were necessary to better understand the rates and processes of exporting biogenic matter from the upper ocean to the interior with regard to detecting oceanographic variabilities in time and space..

The main objective of measuring particle fluxes to the interior of the moderate North Atlantic Ocean at the NABE site by time-series sediment trap array was to understand the magnitude and composition of biogenic particle fluxes throughout a year, in particular during a bloom, and to determine the seasonal variability of mass flux in time and space. Furthermore, we wanted to model the rates and processes of the export of biogenic matter produced in the surface layers to the ocean interior, particularly by comparing changes in the chemistry associated with the 1989 spring bloom to the variabilities in particle fluxes in the ocean interior during the same period.

Our successful field experiment and subsequent laboratory analyses have provided a large body of data that have begun to serve the NABE research community as the basis of many studies (e.g. Altabet *et al.*, 1991; Honjo and Manganini, 1992 and many others in preparation). This report details the analytical results of the biogenic component of fluxes from the experiment with annotation on the analytical methods. We hope this report will be useful as the basis of further investigations of the biogeochemical cycles in the North Atlantic Ocean.

METHOD

Deployment of Sediment Traps and Mooring Arrays

Location, depths and timing.

Two deep ocean mooring arrays were deployed at about 34°N (depth to seafloor: 5,261 m and 5,083 m, for phase 1 and 2) and 48°N (depth to seafloor: 4,418 m and 4,451 m). The approximate locations of sediment trap mooring stations are illustrated in Figure 1. Table 1 gives more detailed information on mooring locations, trap depths and names of ships that were used for deployment and recovery. Three PARFLUX Mark 7G-13 time-series sediment traps with 13 rotary collectors on each were deployed on both moorings for a total of 6 traps. At each of the stations, traps were moored at approximately the same depth relative to the surface and the sea-floor (for the deepest trap); 1 km and 2 km from the surface and 0.7 km above bottom (abbreviated as 0.7 km a.b.) Figure 2 portrays the spatial relationships among the 6 time-series traps.

Arrays were deployed in March and April 1989, recovered and redeployed in September 1989, and totally recovered in April 1990 (Table 1). During the 376-day deployment (including 20 days of hiatus in the middle), each sediment trap was opened and closed 26 times, providing continuous time-series sampling at 14-day intervals, except for two periods. Table 2 lists open/close schedules for which all the traps were uniformly programmed during the experiment. An independent monitoring mechanism installed with each trap (Honjo and Doherty, 1988) confirmed that the entire program was executed correctly and on schedule.

Time-series sediment traps.

Each sediment trap had an aperture of 0.5 m^2, covered by baffles with 25 mm-diameter cells with the aspect ratio of 2.5. The included cone angle was 42 degrees and the structural frame was built of welded titanium The opening and closing of all 6 traps was synchronized with an error of less than one minute. The sample containers, 13 for each trap, were filled with *in situ* deep sea water were collected by a 30 liter Niskin bottle prior to the deployment (Table 4). Analytical grade formalin

(S. Wakeham; personal communication, 1988) was added to make a 3% solution buffered with 0.1% sodium borate (Table 4). Each of the 13 sample containers was completely filled with this sea water solution with preservative before the deployment of a trap. Individual sample containers were mechanically sealed from the ambient water before and after each collecting period (Honjo and Doherty, 1988). The specifications of the PARFLUX Mark 7G-13 are presented in Table 3.

Mooring array

The mooring design was based on the PARFLUX Sediment Trap Mooring Dynamics Package that has been used by us since 1979 (Honjo *et al.*, 1992). Figure 3 illustrates the outline of the mooring that was deployed at the 48°N 21°W station during phase 1 as an example. (A detailed design, parts listing and tension calculation of the NABE mooring array is available in Manganini and Krishfield, 1992, Cruise Report). The arrays were designed to maintain an average of 180 kg of vertical tension throughout the tautline, with a total buoyancy of 1,114 kg that was balanced with a 1,590 kg (in-water weight) cast-iron anchor. Sediment traps were attached to a mooring in-line with three 1-m polyethylene-jacketed bridles. The automatic collection mechanism (Honjo and Doherty, 1988) of the 6 sediment traps worked flawlessly throughout the duration of the experiment and provided us with a total of 156 samples each of which represents an individual key to the time-space matrix for the NABE experiment.

Although the recording was not complete, current meters and thermistors that were deployed 1.2 m below the three sediment traps at the 48°N 21°W station (Fig. 3) (Honjo *et al.*, 1989, Cruise Report) recorded no significant turbulence, and currents were generally less than 5 cm sec^{-1} throughout the year-long deployment. These current meter data were consistent with the reported results of the TOPOGULF Experiment along 48°N (IFREMER, 1987; De Verdiere, 1989). Model calculations obtained from the current record that applied to our mooring at the 34°N and 48°N stations indicated that the traps tilted less that 1° from the vertical during the period of measurement. No significant statistical relationships were found between total flux, particle size groups, particle composition, current direction or strength.

Laboratory Analysis

Pre-analysis treatment of samples

We measured the pH in supernatant in sample containers immediately after recovery of traps (Manganini and Krishfield, 1992, Cruise Report). Sample containers were then refrigerated on board at approximately 2 to 4° C. Particle samples in (original) 250 ml, polyethylene centrifuging sample containers were transported to Woods Hole under refrigeration at approximately 1° to 2° C. We identified no swimmers from all samples collected by our experiment. The impact of swimmers, if any, was relatively small; it appears that they were all included with the >1 mm fractions.

Supernatant analysis

In the shore laboratory, first the liquid in a sample container was decanted and then filtered through a 0.45 μm pore size Nucleopore™ filter leaving approximately 1/3 of the original volume. About 50 ml of filtered liquid was then analyzed for total N, NO_2, NO_3, NH_4, P, PO_4 and SiO_2 using an automatic nutrient analyzer (e.g. Grasshoff *et al.* 1983). We regarded all excess quantities above the ambient concentration as being dissolved from the trapped particles while stored *in situ* before the recovery and added to the particle fluxes after being stochastically converted to solids using the calculation described later (Tables 13 and 14). The remaining liquid in the sampling containers was used as rinse water in the processing of the particulate portion in each specific sample. When additional rinse water was required during the course of analysis, for example, for sample splitting we used filtered and buffered deep Sargasso Sea water containing 3% formalin.

Water sieving

Particle samples were water-sieved through a 1-mm Nitex™ mesh. This was necessary to maintain precision during splitting of the major portion of the sediment that was <1 mm. Common particles in the >1 mm fraction were large aggregates and fragmented gelatinous zooplankton. A sample caught in the 1 mm mesh was then re-suspended in the original seawater, stirred gently and poured onto a grid-printed, 47-mm Nucleopore™ filter with 2-μm pore size, while applying

gentle vacuum suction. While a sample on a filter was wet, the filter with the >1 mm fraction was cut into 4 equal pieces along the printed grid by a Teflon™-coated blade; each aliquot was then immediately put back into the filtered original water for storage. When a >1 mm sample was too small to split, it was dried and homogenized by pulverization.

Sediment that passed through the 1 mm mesh was further water-sieved through a 62 μm Nitex™ sieve. Each fraction was split into 1/4 aliquots and then into 1/40 aliquots by a rotating wet-sediment splitter with 4 and 10 splitting heads (Honjo, 1980). The average error during the splitting of NABE samples into 4 or 10 aliquots was 3.7% for the <1 mm fraction. Wet splitting of the trap-collected sample is justified for multi-disciplinary research including biocoenosis studies. Once particle samples are dried, each becomes inseparable and unidentifiable. Consequently, biocoenosis research such as picking up foraminifera tests or identifying diatom frustules becomes impossible.

Total dry mass measurement

Dry mass was determined by weighing two 1/4 aliquots of >1 mm (whose flux was usually insignificant) and three 1/10 aliquots of <1 mm samples on pre-weighed 47 mm, 0.45 μm Nucleopore filters. Before weighing, the samples were rinsed 3 times with distilled water, dried in an oven at 60° C for 24 hours and cooled in a desiccator for 4 hours. Total flux was calculated from dry weight of the above aliquots divided by aperture area of the trap and the time it was opened.

Sedimentary component analyses

The dried sample was pulverized and homogenized, then the two size fractions were recombined proportionally and analyzed with respect to concentrations of:

a) Carbonate: as $CaCO_3$
b) Biogenic Opal
c) Organic carbon, nitrogen and hydrogen in the decalcified fraction
d) Phosphorus

Carbonate content was determined by a method based on a vacuum-gasometric technique develop. d by Ostermann, *et al.* (1989). A preweighed sample

is introduced into a sealed reaction vessel containing concentrated phosphoric acid. The pressure due to the evolution of CO_2 gas is proportional to the carbonate content when calibrated with appropriate standards and was recorded by a transducer. The results were calculated and reported as carbonate percent in the total sample.

Biogenic opal was estimated from particulate, reactive Si, selectively leaching decalcified samples in a sodium carbonate solution (Eggimann, *et al.*, 1980) and converting the Si content to SiO_2 fluxes. A preweighed sample of approximately 10 mg along with 10 ml of 1 M Na_2CO_3 was sealed in a Teflon™ container. The samples were placed in a shaker bath at 90°C for 3 hours and then filtered through a 47-mm-diameter, 0.45 μm pore size Nucleopore™ filter using an all-plastic filtering apparatus. The filtrate at room temperature was neutralized with 0.2 N HCl using methyl orange as an indicator. After appropriate dilution, content of Si was determined spectrophotometrically (Strickland and Parsons, 1972). The Si content was then converted to SiO_2 and reported as particulate opal flux.

Reactive (biogenic) phosphorus content was determined by the Solorzano and Sharp method that was based on the dissolution of phosphorus by an acid after ashing, using $MgSO_4$ as an oxidant. A preweighed sample was placed into a glass centrifuge tube along with 2 ml of 0.017 M $MgSO_4$ and was dried at 90°C. The centrifuge tube containing the sample was ashed at 500°C for 2 hours. After cooling, 5 ml of 0.2 M HCl was added and, with the centrifuge tube capped, was heated at 80°C for 30 min. At room temperature, 5 ml of distilled H_2O with one ml of reagent (Strickland and Parsons, 1972) was added and the centrifuge tube was shaken in a vortex shaker, then centrifuged. The concentration of phosphorus was determined spectrophotometrically in the supernatant and the results were reported as particulate opal flux.

Preweighed samples on precombusted glass fiber filters were decalcified using 1N phosphoric acid. Organic carbon, nitrogen and hydrogen were analyzed using a Perkin-Elmer Elemental Analyzer Model 240C on the decalcified samples.

Using the method that was applied in this paper, the lithogenic particles were too small to detect and were usually within the analytical error.

Restoration of dissolved components to particulate flux

The dissolution of collected particles in a bottle may occur as soon as particles arrive in the bottle while it is open, or later when it is sealed. Assuming that all dissolved portions remained in the recovered bottle, we restored the dissolved components of Si, P and N by analyzing the supernatants in sample bottles. We assumed that the elevated concentration above the sea water initially used to fill the bottles was caused by dissolved components. During the deployment of a trap, the sample bottles were open to the water column only for the duration of collecting periods. While a bottle was open, the bottle water which was placed in the bottle before deployment is exchanged with ambient water. In case the nutrient concentration of the initial bottle water is not equal to that of the ambient water, a correction had to be made; we assumed that one half of the initial water was diluted by the ambient water while the bottle was open (Tables 4, 5-a and 5-b). In practice, the effect on calculating particle flux by the difference of nutrients in the initial sea water was within analytical error.

Si and P concentrations in the final bottle water are at least twice the water column concentration and in most cases an order of magnitude higher, as indicated in Tables 5-a and 5-b. NO_3 concentration in the bottle water was about equal to or less than the concentration in the initial bottle water (Tables 5-a and 5-b). We report total N without correction by adding the dissolved component.

We define the terms and formula for dissolved component fluxes as follows:

Initial Bottle Water Concentration

The concentration of nutrients in water that was put into a sample bottle before deployment.

Water Column Concentration

The concentration of nutrients in μg-at kg^{-1} in the water column at each station at each depth of each trap (Table 4). We applied following data set: Honjo *et al.*, 1989 (Cruise Report); De Baar, 1990 (Data Report); Slagle and Heimerdinger 1991 (Data Report)

Final Bottle Water Concentration

The concentration of nutrients in the liquid portion of a sample bottle after recovery. Same as "dissolved" in Tables 13 and 14.

Dissolved Components

We assumed the excess level above ambient water column nutrients concentration were added by dissolution of particles.

Total Components

Sum of particulate and dissolved components (Tables 13 and 14).

Formulae

1. Weight of Dissolved Component = (Final Bottle Concentration) – (Water Column Concentration) $\times \dfrac{250 \text{ ml}}{1000\text{ml}} \times$ atomic mass

2. $$\text{Dissolved Component Flux} = \frac{\text{Weight Dissolved Component}}{\text{time} \times \text{aperture area } (0.5 \text{ m}^2)}$$

3. Percent Flux =

$$\frac{\text{Dissolved Component Flux}}{(\text{Dissolved Component Flux}) + (\text{Particulate Component Flux})} \times 100$$

Flux Calculations

We describe particle flux in four timescales in this report: annually, per episode (pre-bloom, bloom and post-bloom; Honjo and Manganini, 1992), per period and daily. Flux per period was obtained by direct measurement during one 14-day open trap period (except for one longer and one shorter period, Table 2). All periods started/ended at 12:00 GST. The annual flux is the flux of particles during 365 days, including all three episodes; pre-bloom, bloom and post-bloom. Each episode was characterized by the quantity of particle fluxes (Honjo and Manganini, 1992) (Fig. 4).

Although the rotating mechanism of the sediment traps worked flawlessly, there were periods where the samples were found to be unusable, or were absent, due to the intrusion of Argentine fish *(Argentina sphyraena)* into the sample bottles, blocking the mouth of the sample bottles, or due to accidental loss of 2 samples during transportation (Fig. 4). Also the NABE trap experiment was interrupted for 20 days in September 1989 for change-over of moorings. Therefore it was necessary to estimate fluxes per episode and per calendar year using averaging methods described below. Annual and episodic fluxes in Tables 7 through 11 were based on this normalized collecting time. Table 6 shows total days and the percentages of sample collection time, actual collecting time and normalized collecting time. Definitions used were:

Sample Collecting Time

The duration of time that samples were collected; does not include hiatus or fish-blocked samples. Total time was different for each trap.

Actual Collecting Time (in days)

The duration of time for the entire collection schedule including hiatus and blocked samples. Total of 378 days for all traps.

Normalized Collecting Time (in days)

Elapsed time as normalized to one year, 365 days.

Formulae

1. Average Flux (mg m^{-2} day^{-1}) =

$$\frac{\text{total weight (mg)} \times \text{aperture of trap } (0.5\ m^2)}{\text{sample collecting time}}$$

2. Percent Actual Collection Time (%) = $\frac{\text{actual elapsed time}}{\text{378 days}} \times 100$

3. Normalized Elapsed Time (days) $= \dfrac{\text{Percent Actual Collection Time} \times 365}{100}$

4. Normalized Period Flux ($g\ m^{-2}\ period^{-1}$) =

$$\frac{(\text{Average Flux mg } m^{-2}\ day^{-1}) \times (\text{Normalized Elapsed Time})}{100}$$

5. Total normalized yearly flux =

(Normalized Pre-bloom Flux) + (Normalized Bloom Flux) + (Normalized Post-Bloom Flux)

6. Normalized Percent Yearly Flux Per Period =

$$\frac{\text{Normalized Period Flux}}{\text{Total Yearly Flux } (g\ m^{-2}\ yr^{-1})} \times 100$$

RESULTS

Annual Particle Flux

Table 7 summarizes total annual particle fluxes and particle fluxes during pre-, post- and bloom episodes. Table 8 (34°N station) and Table 9 (48°N station) show fluxes of critical sedimentological and biogeochemical components during each episode and their proportions in the annual fluxes.

Annual mass flux normalized to 365 days at the 34°N station, 2 km and 0.7 km a.b. was 22.4 and 21.2 $g\ m^{-2}\ yr^{-1}$ respectively. At the 48°N station the total flux from equivalent levels was 26.9 and 26.2 $g\ m^{-2}\ yr^{-1}$, respectively (Table 7). These were compared with a 6-year mean annual flux measured near Bermuda (32°N 64°W); which was 16.3 $g\ m^{-2}\ yr^{-1}$ (1 km a.b.) (Deuser, 1986). Annual fluxes measured from 1983 to 1986 in the Nordic Seas ranged from 28.4 (76°N 11°E) to 7.2 $g\ m^{-2}\ yr^{-1}$ (78°N 01°E) (Honjo, 1990).

Total annual fluxes at the 1-km depth at the 34°N and 48°N stations were 19.4 and 19.9 g m^{-2} yr^{-1} respectively and were smaller than the annual mass fluxes measured at the two deepest traps. At the 34° station this was attributed to the intrusion of a fish during JD 119 period (mid-date, April 29, 1989) that accidentally plugged the lower end of the trap (Fig. 4). As shown in Table 8 (34°N 21°W station) and Table 9 (48°N 21°W station), as well as in Figure 6, calcium carbonate ($CaCO_3$) was the largest component of settling particles. Particulate organic matter (POM) determined by combustion loss and biogenic opal followed. At 2 km deep, the concentrations of $CaCO_3$, POM and opal were 61.8, 28.8 and 9.1% at the 34°N station and 55.3, 23.0 and 21.9% at the 48°N station, respectively. At 0.7 km a.b., the concentrations of $CaCO_2$, POM and opal were 60.8, 29.6 and 9.4% at the 34°N station and 58.8, 19.9 and 21.4% at the 48°N station, respectively.

Variability of Particle Fluxes by Period

Tables 13 (34°N) and 14 (48°N) show the seasonal evolution of total particle fluxes, fluxes of particles in two sizes and basic sedimentational and biogeochemical constituents per period. Particle fluxes during each period are plotted with time in Figures 4 and 5. The proportions of constituents in total flux is illustrated in Figure 6. An episode of high particle flux (particle bloom) was observed during springtime at both stations (Fig. 4).

We defined a particle bloom episode as a rapid and continuous increase in particle flux to a peak or peaks, followed by a rapid and consistent decrease to the background flux (Honjo and Manganini, 1992). The boundaries of each episode were first defined at 1 km; then these boundaries were shifted to one period later for the 2-km depth; and then again to one more period later for the 0.7-a.b. depth. At both stations and at all depths no complete spring bloom was observed during this experiment; when the first set of sediment traps was deployed the 1989 spring bloom was already in process; the 1990 bloom was still continuing when the second-phase traps were recovered. We combine years 1989 and 1990 to show one complete bloom cycle as illustrated in Figure 4.

At both stations, a spring particle bloom consisted of two or three outstanding peaks separated by about one month (Figs. 4 and 5). There was a relatively long duration between the two blooms, when the particle fluxes were far smaller and

more stable with time. These periods can be divided into pre- and post-particle-bloom episodes. Distinction of the three episodes involved subjective judgment.

Variability of Particle Fluxes by Depth

The succession of flux variability which is seen in a graph where all periods are plotted with time at shallower depths, was imprinted at deeper levels with or without time-lags. As illustrated in Figures 4 and 5, by comparing the "peak-valley" succession within the 1990 spring bloom at the 34°N station in 1990, for example, the penetration of total flux from 1,248 m to 1,894 m was shifted for one sampling period (14 days). On the other hand, also as illustrated in Figure 4, the peak-valley pattern of fluxes and components during the spring bloom observed at 1,894 m in the spring of 1990 at the 34°N station was repeated at 4,391 m without apparent delay within the 14 days of sampling resolution. At the 48°N station in spring 1989, the later portion of the bloom at 1 km was not as elaborately represented as at the two deeper traps. Peak fluxes found during the bloom at the 2-km trap were fused into a single broader peak at 3,718 m deep. The relatively short arrival time of particles to subsequently deeper traps suggested a rapid and nondiscriminatory settling of particles at both stations.

There was a third but less outstanding peak of particle flux at the end of the post-bloom period at the 48°N 21°W station in JD 262 period (September 19, 1989). This small peak, characterized by relatively enriched organic matter, was repeated at all depths, arriving without delay at the deeper traps. No such similar peak was observed at the 34°N station during its post-bloom period (Fig. 4).

Fluxes of Sedimentary Components

The average fluxes of sedimentary components and their percentage in the total annual flux in each episode: $CaCO_3$, opal, particulate organic carbon, nitrogen and particulate reactive phosphorus are given in Tables 8 and 9. Tables 13 and 14 show the fluxes of $CaCO_3$, particulate organic carbon, nitrogen (in "b-series" tables), SiO_2 as opal (in "c-series" tables) and particulate phosphorus (in "d-series" tables). The proportion of dissolved SiO_2 and P with particulated SiO_2 and P are shown in Tables 13 and 14, in percent or ppm by dry weight (in "c-series" and "d-series" tables).

Ratios of Critical Biogeochemical Elements

The molar ratios between a several pairs of critical biogeochemical elements during each period and depths were calculated as illustrated in the "e-series" of Tables 13 and 14.

Ca	(in biogenic calcite and aragonite)	*vs.*	Si (in opal)
C	(total organic)	*vs.*	N (organic)
C	(total organic)	*vs.*	P (total reactive)
N	(organic)	*vs.*	P (total reactive)
C	(total organic)	*vs.*	Si (in opal)

In particle fluxes, the terminal ratio is a constant ratio of fluxes of two chemical species, which is attained as particles settle through the water column. Terminal ratios were observed in specific combinations of elemental fluxes. As two particulate chemical compounds settle, the ratio of their molar fluxes changes as depth increases, but generally reaches a constant ratio at a depth which may vary from area to area. The terminal ratio, however, does not vary with season, but may differ geographically.

As an example, variability of ratios between organic carbon (C_{org}) *vs.* carbon in $CaCO_3$ (C_{inorg}) at the 48°N station at each depth and period, are illustrated in Figure 7. C_{org}/C_{inorg} ratios varied substantially in the shallow levels, but reached more consistency at 4,418 and 4,451 m. The C_{org} vs. C_{CaCo_3} ratio per each period became 0.57 and 0.54 at 0.7 km a.b. at the 34°N and 48°N stations, respectively, with a small standard deviation from the mean (Fig. 7). Other examples are that the terminal ratios of Ca and Si at the 34°N and 48°N stations were 4 and 2, respectively, and the terminal ratio of C and P at the 34°N station was 150 (Fig. 8).

Changes of critical biogeochemical ratios by episode are illustrated in Figure 8. The C/P ratio, for example, reached the terminal ratio at 150 at 0.7 km a.b. The C : N : P molar ratio at the deepest trap was 154 : 18 : 1 at 34°N station and 148 : 18 : 1 at the 48°N station (Table 12).

ACKNOWLEDGMENTS

We are grateful to the Joint Global Ocean Flux Program for providing the opportunity to conduct this experiment. We thank Richard Krishfield for assisting in all NABE mooring deployment and recovery cruises. Kenneth Doherty contributed to the success of the program through continuously improving the reliability of the time-series sediment traps. The professionalism of the officers and crew of R/V Atlantis II, R/V Endeavor and HMS Charles Darwin made this difficult deployment of complex mooring arrays, often in high seas at mid-night, sometimes in snowstorms, successful, resulting in all instruments being recovered without incidents. McLane Research Laboratories, Inc. provided all spare parts for the Mk 7G-13 sediment traps and moorings without charge. Katherine Brown expertly laid out the tables in the Technical Report. This program was supported by National Science Foundation under Grant Number OCE 88-14228 (JGOFS/NABE program).

REFERENCES

Altabet, M. A., Deuser, W. G., Honjo, S., and Stienen, C., 1991. Seasonal and depth-related changes in the source of sinking particles in the North Atlantic, *Nature*, **345**: 136-139.

Bradshaw, J. S., 1959. Ecology of living planktonic foraminifera of the North and Equatorial Pacific ocean. *Cushman Found. Foram. Res., Contr.* **10**(2), 25-64.

De Baar, W. J. W., 1990. *Data Report; Joint Global Ocean Flux Study, First Report: R. V. Tyro, Leg 1, Den Helder – Reykjavik – Funchal, 31 July to 11 September 1989*. SOZ Data Report 1990, Nederlands Instituut Voor Onderzoek der Zee. 138 pp.

Deuser, W. B., 1986. Seasonal and interannual variations in deep-water particle fluxes in the Sargasso Sea and their relation to surface hydrography, *Deep-Sea Research*, **33**: 225-246.

De Verdiere, C., 1989. Mesoscale variability transition from the Western to the Eastern Atlantic along 48 degree N, *J. Phys. Oceanogr.*, **19**(8): 1149-1170.

Eggimann, D. W., Manheim, F. T., and Betzer, P. R., 1980. Dissolution and analysis of amorphous silica in marine sediments. *Jour. Sediment Petrol.* **50**: 215-225.

Grasshoff, K., Ehrhardt, M, and Kremling, K., (eds.), 1983. *Method of Sea-Water Analysis*. Weinheim, Verlag Chemie, 419 pp.

Honjo, S., 1980. Material fluxes and modes of sedimentation in the mesopelagic and bathypelagic zones, *Journal of Marine Research*, **38**: 53-97.

Honjo, S., 1990. Particle Fluxes and Modern Sedimentation in the Polar Oceans, Chapter 12 *in* Smith, W. O., Jr., (ed.), *Polar Oceanography*, Academic Press, New York, Vol. II, p. 322-353.

Honjo, S. and Doherty, K. W., 1988. Large aperture time-series sediment traps; design objectives, construction and application. *Deep-Sea Research*, 35(1): 133-149.

Honjo, S. and Manganini, S. J., 1992. Annual Biogenic Particle Fluxes to the Interior of the North Atlantic Ocean; Studies at 34°N 21°W and 48°N 21°W. *Deep-Sea Research* (accepted).

Honjo, S., Manganini, S. J., and Krishfield, R., 1989. Cruise Report: JGOFS Leg 1, International Study of the North Atlantic Bloom, R/V Atlantis II Voyage 119.2, Funchal to Reykjavik, March/April 1989. *WHOI Technical Report,* WHOI-89-22, Woods Hole Oceanographic Institution, 28 p.

Honjo, S., Spencer, D. W., and Gardner, W. D., 1992. Sediment trap Intercomparison Study in the Panama Basin, *Deep-Sea Research,* 39: 333-358

IFREMER, 1987. Long term current measurements along 48 degree N in the Central North Atlantic. TOPOGULF Cruise 2; Current meter measurements; Data report.

Manganini, S. J. and Krishfield, R., (in preparation) Cruise Report: JGOFS Trap Deployment Legs 2 and 3, International Study of the North Atlantic Bloom, R/V Endeavor, Voyage 203 and HMS Charles Darwin 45B, , *WHOI Technical Report,* Woods Hole Oceanographic Institution.

Okada, H. and McIntyre, A., 1979. Seasonal distribution of modern coccolithophores in the western North Atlantic Ocean. *Marine Biology,* 54: 319-328.

Ostermann, D. R., Karbott, D., and Curry, W. B., 1990. Automated system to measure the carbonate concentration of sediments. WHOI Technical Report, WHOI-90-03.

Slagle, R. and Heimerdinger, G., 1991. *Data report; North Atlantic Bloom Experiment April-July 1989, Process Study Data Report P-1, U. S. Joint Global ocean Flux Study.* NODC/U.S. JGOFS Data Management Office, Woods Hole Oceanographic Institution, Woods Hole, MA 02543, 315 pp.

Solarzano, L. and Sharp, J. H., 1980. Determination of total dissolved phosphorus and particulate phosphorus in natural waters. *Limnol. Oceanogr.* 15(4): 754-758.

Strickland , J. D. H. and Parsons, T. R., 1972. *A Practical Handbook of Seawater Analysis.* Fisheries Research Board of Canada, Bulletin 169, 2nd edition, Ottawa, 310 p.

EXPLANATION OF FIGURES

Figure 1 Location of NABE time-series stations.

Figure 2 Approximate transect profile along 21°W. Solid triangles along moorings indicate approximate depths of time-series sediment traps deployed in 1989 and 1990.

Figure 3 Schematic diagram of the mooring deployed at the 48°N 21°W station. For the mooring that was deployed at the 34°N 21°W station, approximately 600 m deeper, extra shots of 3/16" wire rope were added between the 2 km and 0.7 km a.b. traps.

Figure 4 Annual variability of mass flux at the 34°N 21°W and the 48°N 21°W stations at 3 depths with distinction of bloom, pre- and post-bloom episodes in 14 days' resolution. The periods with 5 days (JD 96 period) and 17 days (JD 148 period) opening normalized to 14-day fluxes for this figure and Figures 5 and 6. The fish symbol indicates the period when an argentine fish was accidentally caught, spoiling the flux data thereafter. *The same species was caught in all three incidents.* "*" indicates sample was lost during transportation. "H" indicates hiatus in deployment due to change of arrays.

Figure 5 Annual variability of the major biogenic components at the 34°N 21°W and 48°N 21°W stations at 3 depths. "H_2O and others" includes water from organic matter (reconstructed from hydrogen flux obtained from elemental analyzer), opaline skeletons and other ignition losses. Trace mass fluxes of lithogenic particles such as clay and air-borne minerals are included in this category. This also applies to Figure 6. The fish symbol indicates the period when an argentine fish was accidentally caught, spoiling the flux data thereafter. "*" indicates sample was lost during transportation. "H" indicates hiatus in deployment due to change of arrays.

Figure 6 Proportion of the major biogenic components at the 34°N 21°W and the 48°N 21°W stations at 3 depths.

Figure 7 Vertical changes of the $C_{org.}/C_{CaCO_3}$ from the spring of 1989 to the spring of 1990 at the 48°N station. Ratios were higher in the shallower depths and varied widely at different times. They decreased with depth, eventually reaching a terminal ratio that was more uniform through all seasons. The insert shows the development of the $C_{org.}/C_{CaCO_3}$ terminal ratio through the pre-bloom, bloom and post-bloom episodes in the same manner as Fig. 8.

Figure 8 Schematic illustration of the change of total flux (upper most) and the ratio between critical biogenic elements during the pre-bloom, bloom and post-bloom episodes in an year (normalized to 365 days) by Julian Days at the 34°N 21°W and the 48°N 21°W stations at 3 depths. Annual averages of fluxes and elemental ratios are given on the right end of each column.

Figure 1

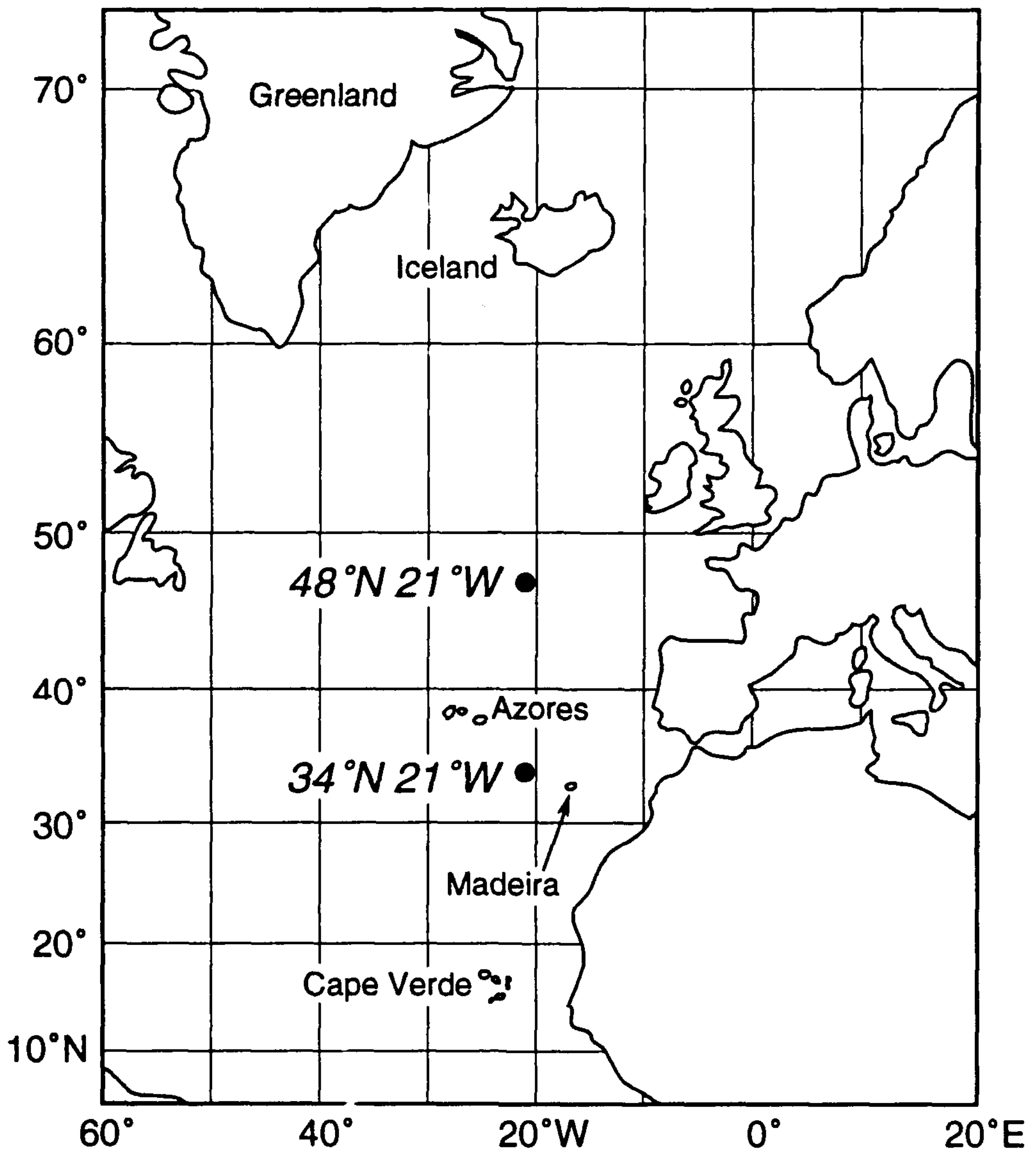

70°
60°
50°
40°
30°
20°
10°N
Greenland
Iceland
48°N 21°W
Azores
34°N 21°W
Madeira
Cape Verde
60°
40°
20°W
0°
20°E

Figure 2

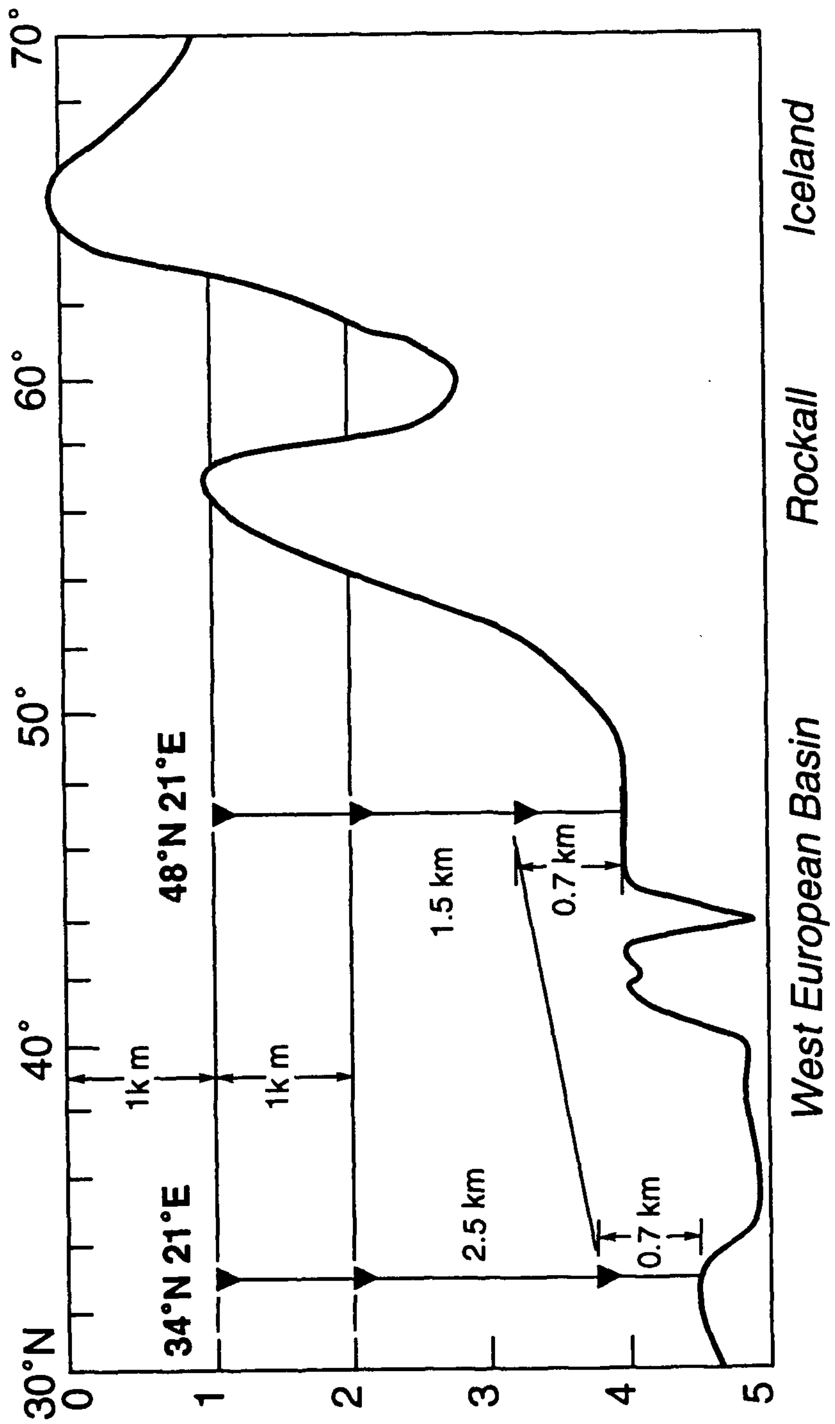

30°N
40°
50°
60°
70°
0
1
2
3
4
5
34°N 21°E
48°N 21°E
1k m
1k m
2.5 km
1.5 km
0.7 km
0.7 km
West European Basin
Rockall
Iceland

Figure 3

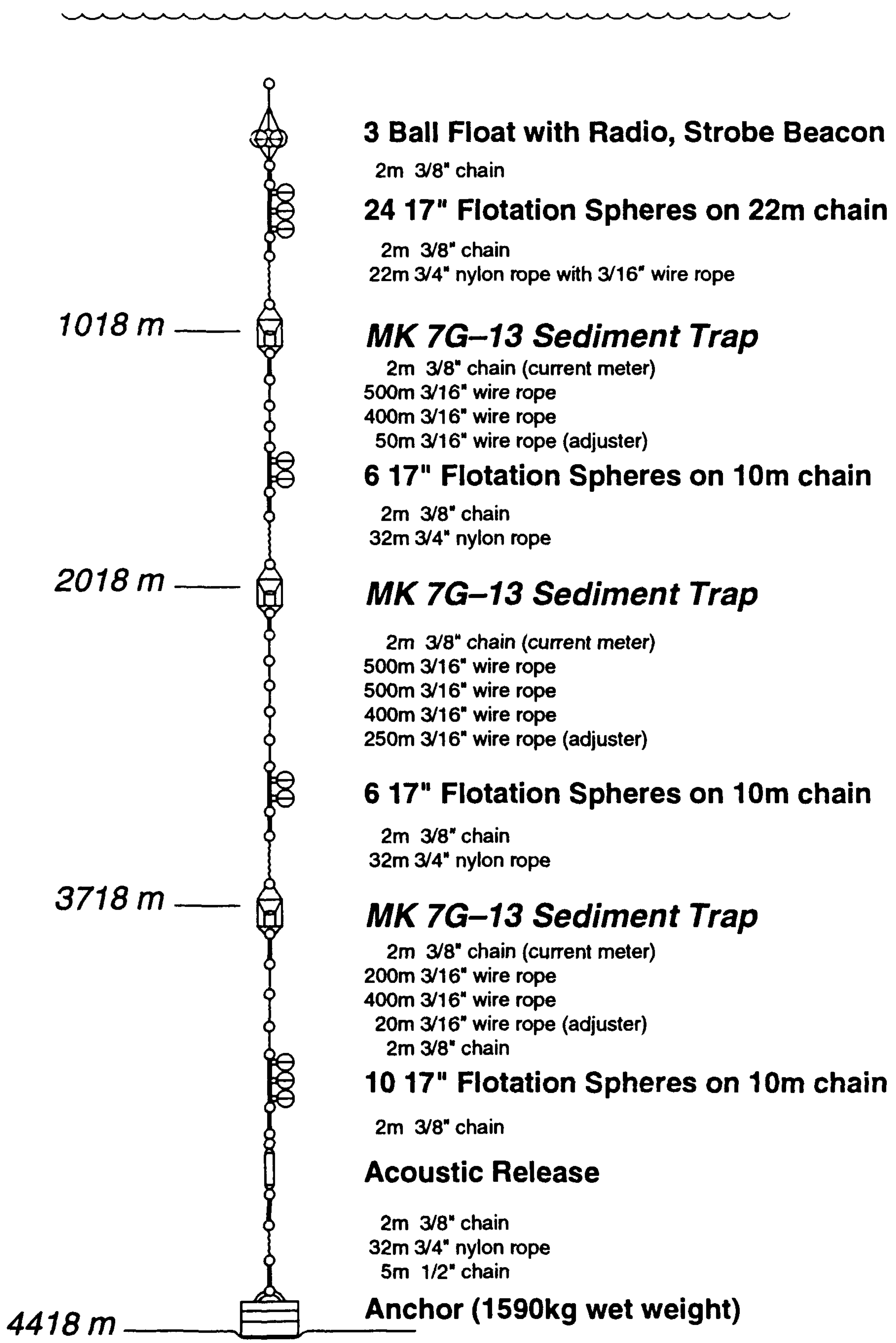
3 Ball Float with Radio, Strobe Beacon
2m 3/8" chain
24 17" Flotation Spheres on 22m chain
2m 3/8" chain
22m 3/4" nylon rope with 3/16" wire rope
1018 m
MK 7G–13 Sediment Trap
2m 3/8" chain (current meter)
500m 3/16" wire rope
400m 3/16" wire rope
50m 3/16" wire rope (adjuster)
6 17" Flotation Spheres on 10m chain
2m 3/8" chain
32m 3/4" nylon rope
2018 m
MK 7G–13 Sediment Trap
2m 3/8" chain (current meter)
500m 3/16" wire rope
500m 3/16" wire rope
400m 3/16" wire rope
250m 3/16" wire rope (adjuster)
6 17" Flotation Spheres on 10m chain
2m 3/8" chain
32m 3/4" nylon rope
3718 m
MK 7G–13 Sediment Trap
2m 3/8" chain (current meter)
200m 3/16" wire rope
400m 3/16" wire rope
20m 3/16" wire rope (adjuster)
2m 3/8" chain
10 17" Flotation Spheres on 10m chain
2m 3/8" chain
Acoustic Release
2m 3/8" chain
32m 3/4" nylon rope
5m 1/2" chain
4418 m
Anchor (1590kg wet weight)

Figure 4

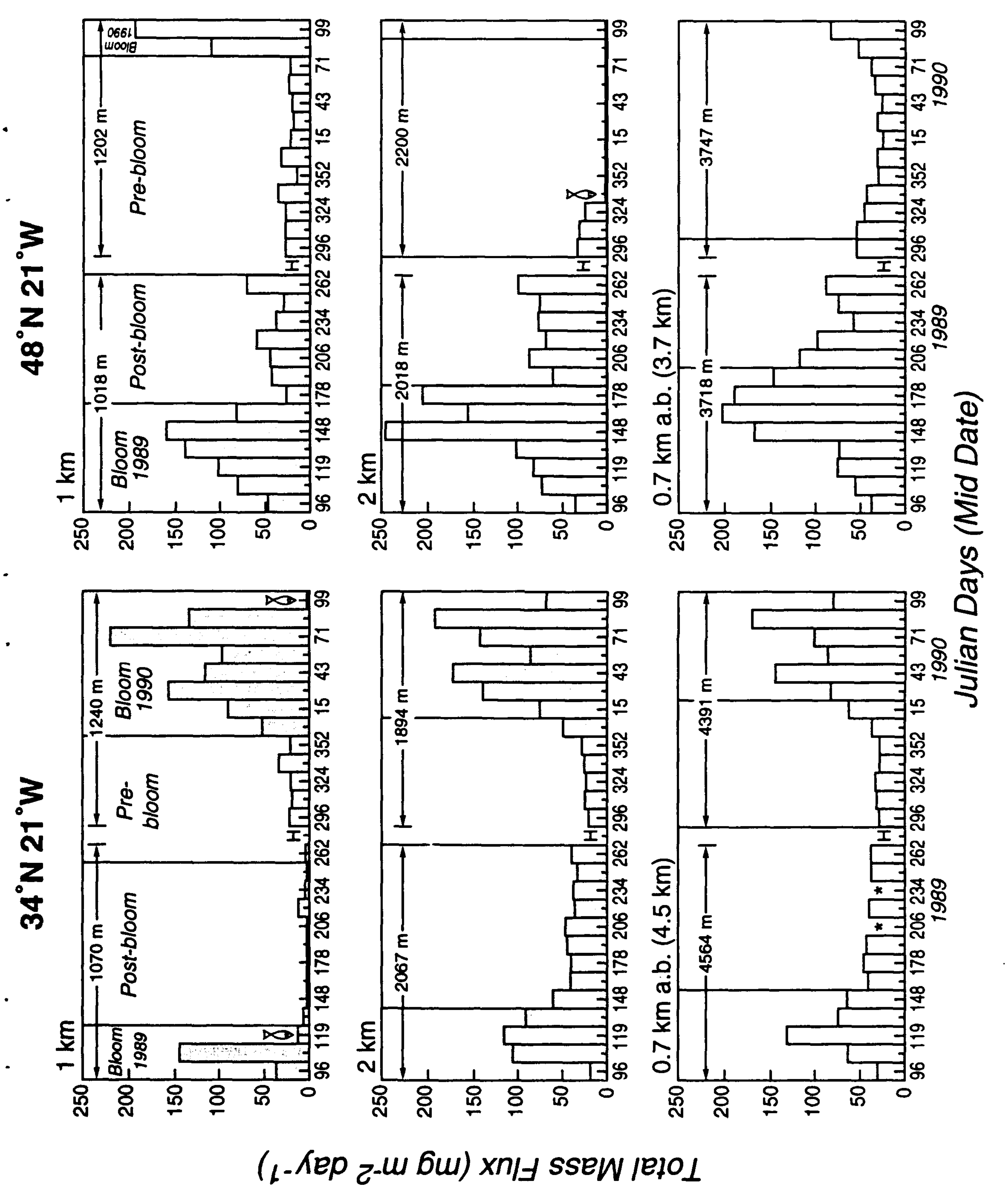

34°N 21°W
48°N 21°W
1 km
2 km
0.7 km a.b. (4.5 km)
0.7 km a.b. (3.7 km)
Bloom 1989
Post-bloom
Pre-bloom
Bloom 1990
1070 m
1240 m
2067 m
1894 m
4564 m
4391 m
1018 m
1202 m
2018 m
2200 m
3718 m
3747 m
96 119 148 178 206 234 262 296 324 352 15 43 71 99
1989
1990
Julian Days (Mid Date)
Total Mass Flux (mg m-2 day-1)

Figure 5

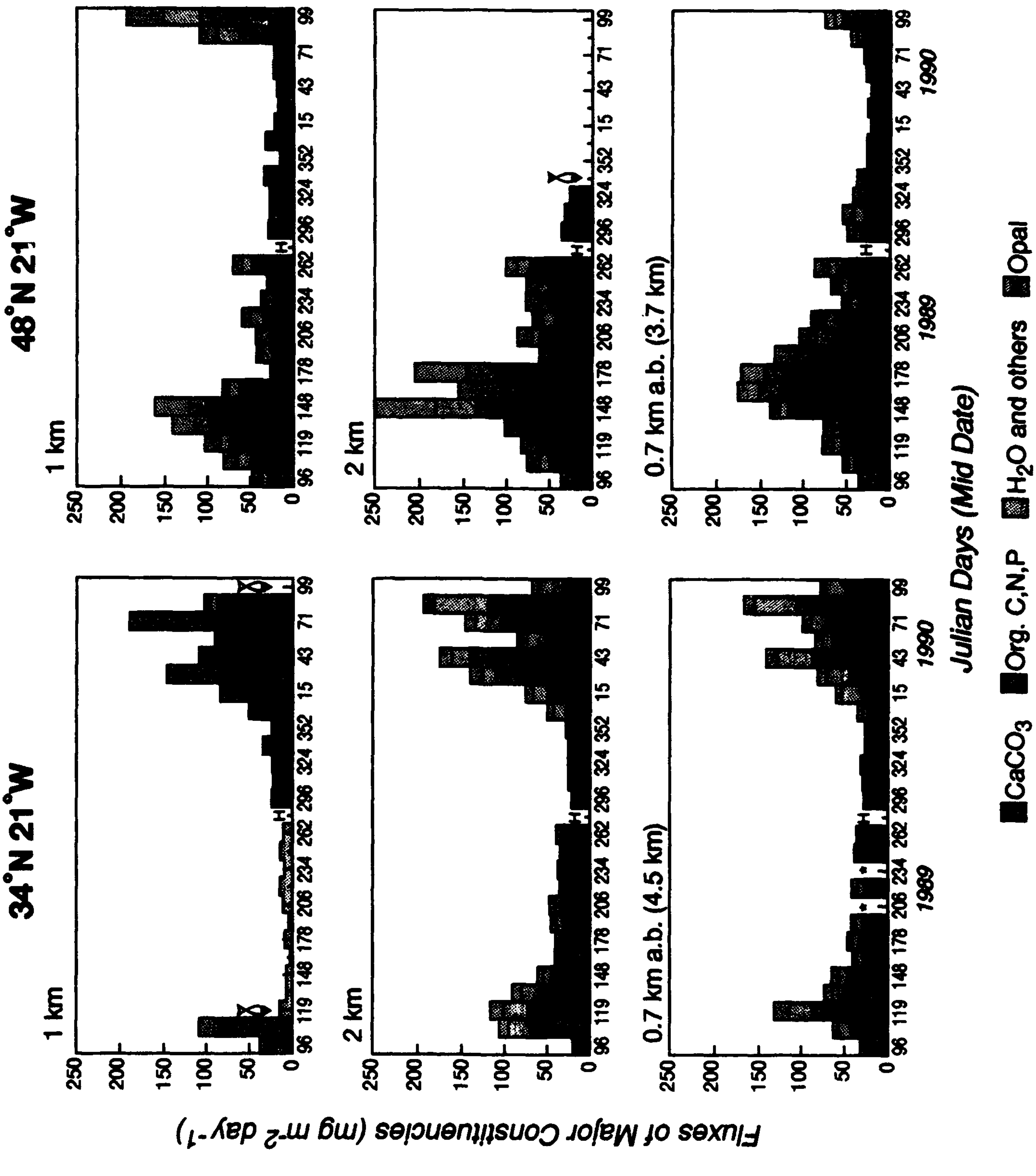
34°N 21°W
48°N 21°W
1 km
2 km
0.7 km a.b. (4.5 km)
0.7 km a.b. (3.7 km)
Fluxes of Major Constituencies (mg m^{-2} day^{-1})
Julian Days (Mid Date)
1989
1990
$CaCO_3$
Org. C,N,P
H_2O and others
Opal

Figure 6

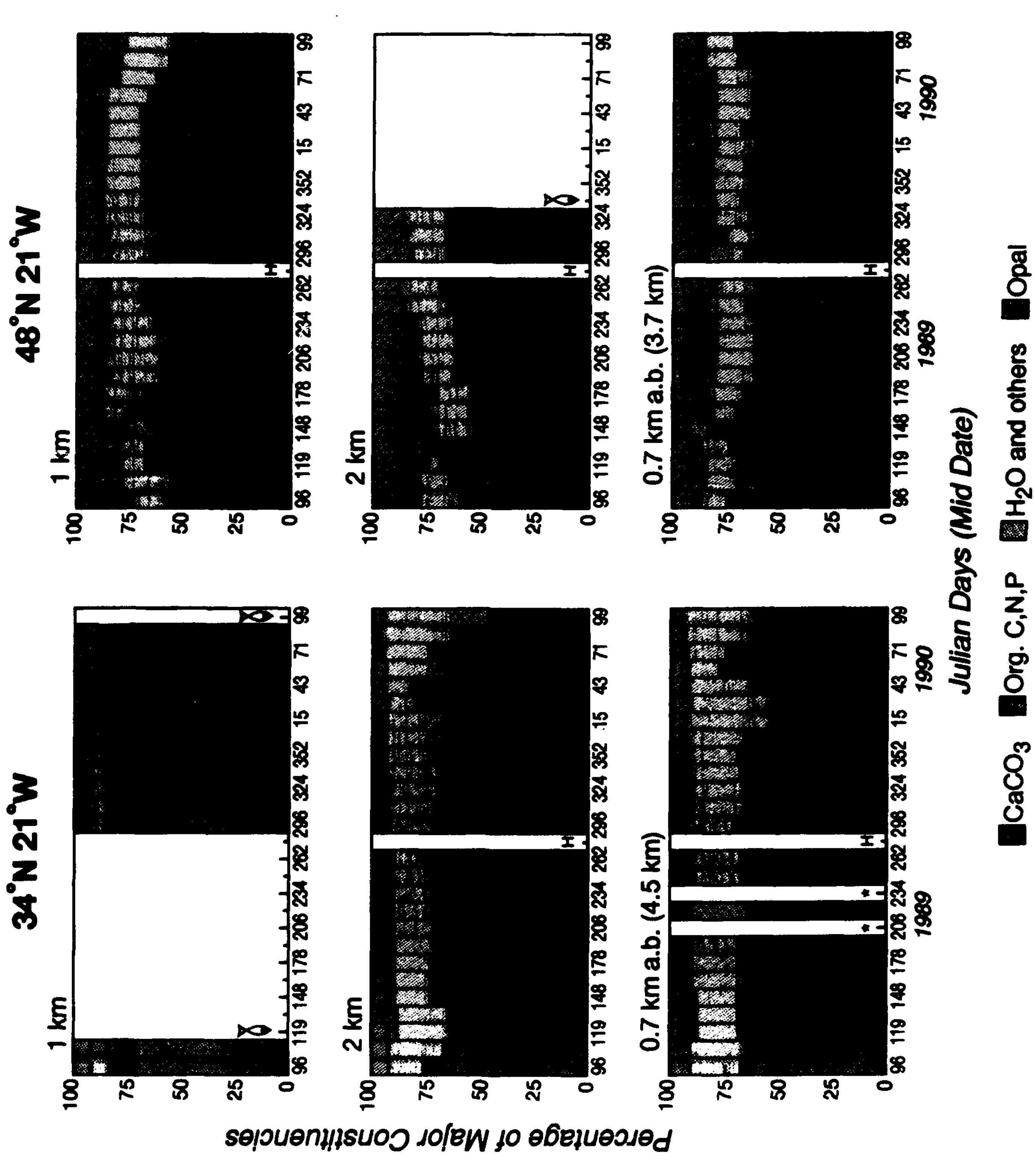

34°N 21°W
48°N 21°W
1 km
2 km
0.7 km a.b. (4.5 km)
0.7 km a.b. (3.7 km)
Percentage of Major Constituencies
100
75
50
25
0
96 119 148 178 206 234 262 298 324 352 15 43 71 99
1989
1990
Julian Days (Mid Date)
CaCO3
Org. C,N,P
H2O and others
Opal

Figure 7

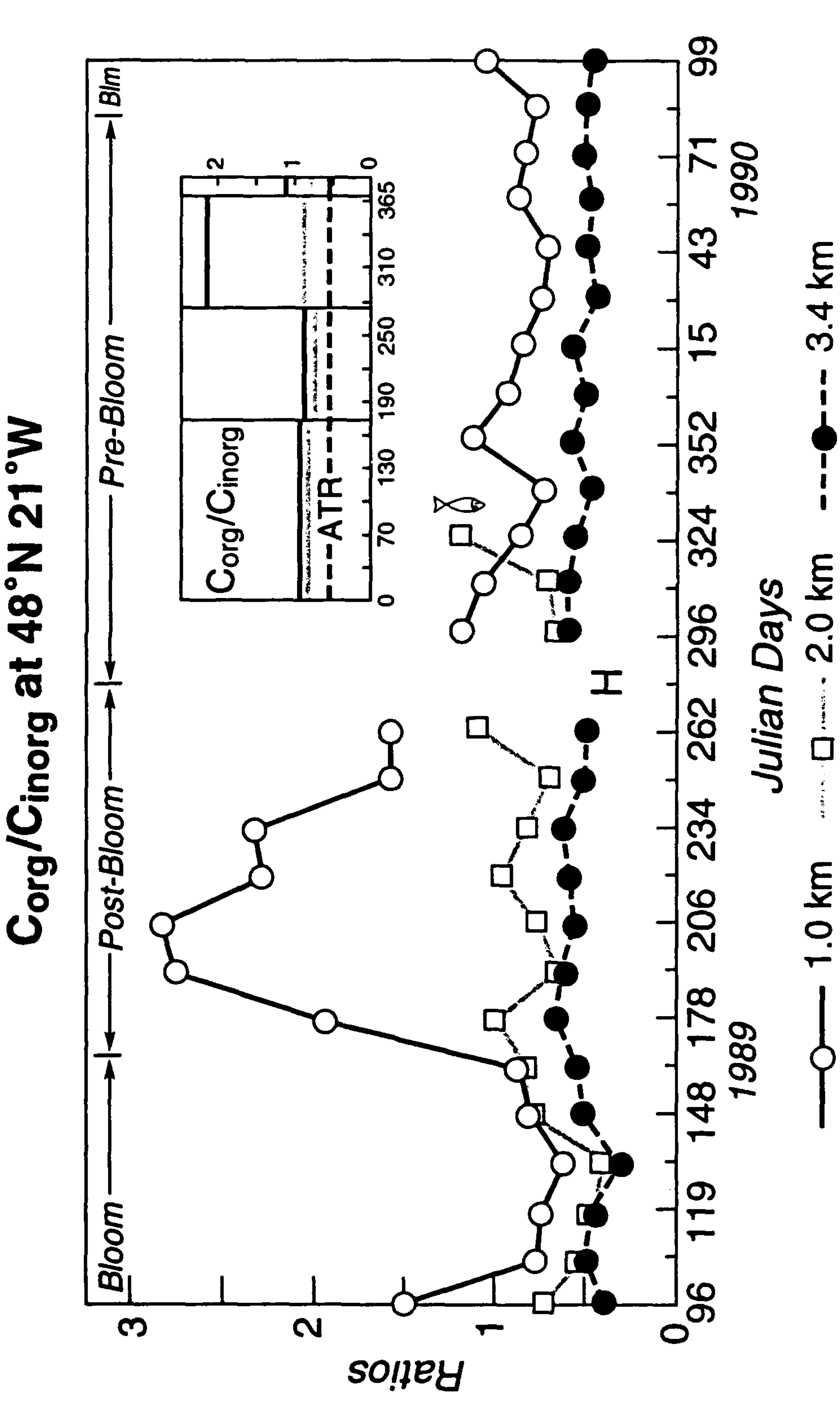

C_{org}/C_{inorg} at 48°N 21°W
Bloom
Post-Bloom
Pre-Bloom
Blm
Ratios
0
1
2
3
96
119
148
178
206
234
262
296
324
352
15
43
71
99
1989
1990
Julian Days
H
C_{org}/C_{inorg}
ATR
0
70
130
190
250
310
365
1.0 km
2.0 km
3.4 km

Figure 8

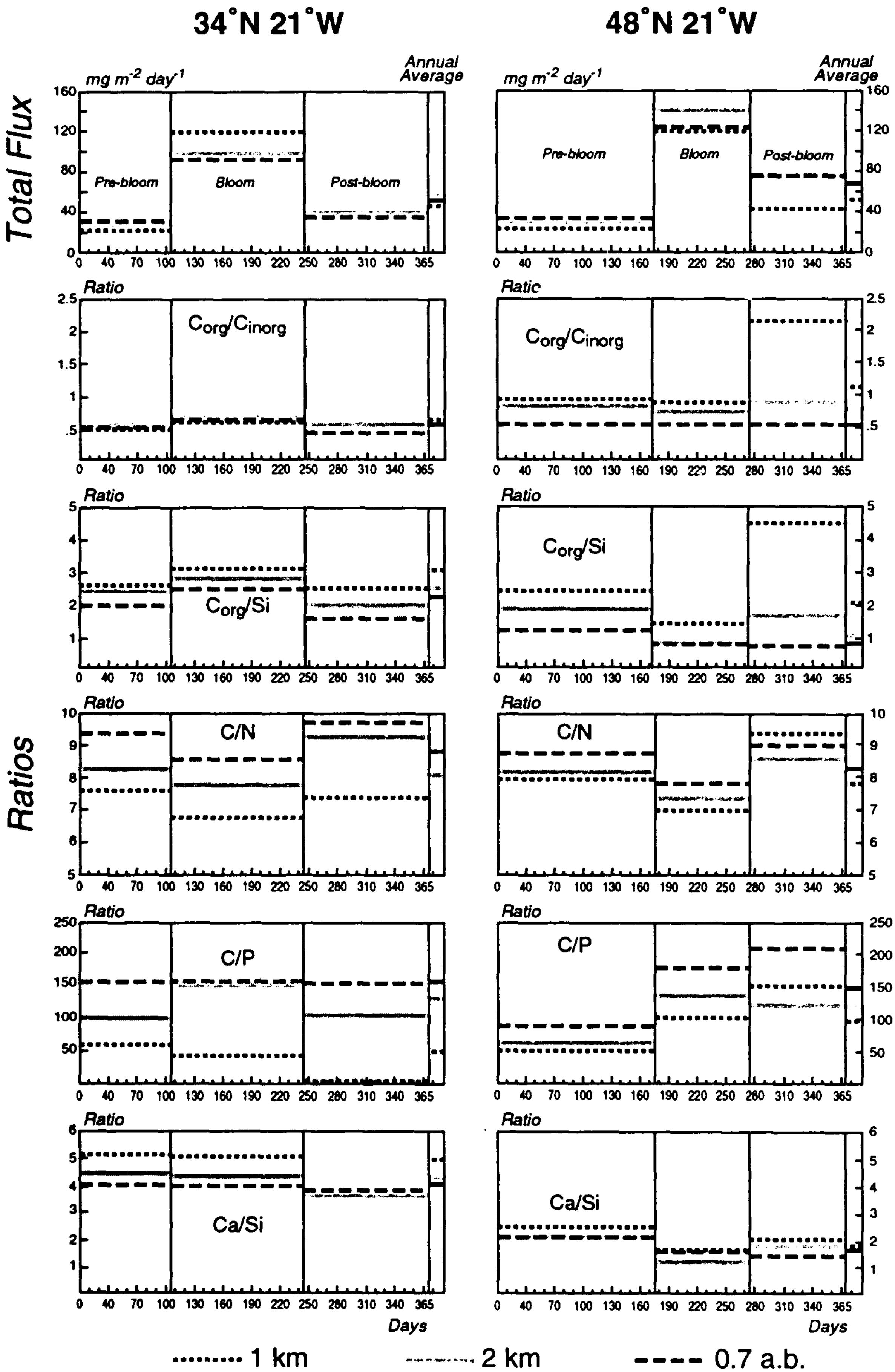
34°N 21°W
48°N 21°W
Total Flux
Ratios
mg m-2 day-1
Annual Average
Pre-bloom
Bloom
Post-bloom
Ratio
Corg/Cinorg
Corg/Si
C/N
C/P
Ca/Si
Days
1 km
2 km
0.7 a.b.

EXPLANATION OF TABLES

Table 1 Mooring stations and trap depths.

Table 2 Synchronized open/close schedule for all traps at the 34°N 21°W and 48°N 21°W stations.

Table 3 Specifications of sediment traps.

Table 4 Location, depth and nutrient concentration of water used for Initial Bottle Water

Table 5 Concentration of dissolved nutrients

Table 5 - a Water used for the 34°N traps

Table 5 - b Water used for the 48°N traps

Table 6 Various times that were used to deliver the lengths of "normalized episodes" and the 365-day calendar year.

Table 7 Summary Table; annual total particle fluxes and total fluxes per episode.

Table 8 Fluxes and proportions (%) of principal sedimentary components per episode at the 34°N 21°W station.

Table 9 Fluxes and proportions (%) of principal sedimentary components per episode at the 48°N 21°W station.

Table 10 Ratios between critical biogeochemical elements at each episode at the 34°N 21°W station.

Table 11 Ratios between critical biogeochemical elements at each episode at the 48°N 21°W station.

Table 12 "Redfield Ratio" (C : N : P, when P = 1) in trapped particles at 34°N 21°W and 48°N 21°W station calculated for each depth and episode. Published Redfield Ratio in living plankton is 106 : 16 : 1.

Table 13 Flux information per period at 34°N 21°W.

Table 13 - 1 contains the following information regarding particle fluxes and their proportions per period (generally 14 days) in the shallow trap (1 km) at 1071 m (Phase 1) and 1248 m (Phase 2) at 34°N 21°W, in sub-tables a – b.

Table 13 -1 - a Size fractions, fluxes and proportion (%), >1 mm and <1 mm after water-sieving.

Table 13 -1 - b Fluxes of calcium, inorganic carbon, organic carbon and organic nitrogen.

Table 13 -1 - c Opal SiO_2 fluxes. SiO_2 was dissolved from the particles after they were trapped and retained in the supernatant of sample container. They were then converted to solid flux (mg m^{-2} day^{-1}), combined with particle flux and reported as SiO_2 in opal (Column 3). Proportions (%) of dissolved particulate per bottle (representing one period) are given in Columns 8 and 9.

Table 13-1 -d Fluxes of reactive phosphorus. P in PO_4 was dissolved from the particles after they were trapped and retained in the supernatant of sample container. They were then converted to solid flux (mg m^{-2} day^{-1}), combined with the particle flux and reported as total organic (reactive) P (Column 3). Concentrations (ppm) of dissolved particulates per bottle (representing one period) are given in Columns 6, 7 and 9.

Table 13 - 1 - e Molar ratios between critical biogenic elements calculated from the fluxes presented in Tables 13-1-b through d.

Table 13 - 2 Information regarding particle fluxes and their proportions per period (generally 14 days) in at the mid-depth trap (2 km) at 2067 m (Phase 1) and 1894 m (Phase 2) at 34°N 21°W in sub-tables a – b. Sub-tables repeat the content explained in Table 13-1-a through Table 13-1-e.

Table 13 - 3 contains the following information regarding particle fluxes and their proportions per period (generally 14 days) at the deepest trap (0,7 km above the bottom) at 4564 m (Phase 1) and 4391 m (Phase 2) at 34°N 21°W in Sub-tables a through b. Sub-tables repeat the content explained in Table 13-1-a through Table 13-1-e.

Table 14. Flux information per period at 48°N 21°W.

Table 14 - 1 contains information regarding particle fluxes and their proportions per period (generally 14 days) in the shallow trap (1 km) at 1071 m (Phase 1) and 1248 m (Phase 2) at 48°N 21°W in sub-tables a – b. Sub-tables repeat the content explained in Table 13-1-a through Table 13-1-e.

Table 14 - 2 contains information regarding particle fluxes and their proportions per period (generally 14 days) in at the mid-depth trap (2 km) at 2067 m (Phase 1) and 1894 m (Phase 2) at 48°N 21°W in sub-tables a – b. Sub-tables repeat the content explained in Table 13-1-a through Table 13-1-e.

Table 14 - 3 contains information regarding particle fluxes and their proportions per period (generally 14 days) in at the deepest trap (0,7 km above the bottom) at 4564 m (Phase 1) and 4391 m (Phase 2) at 48°N 21°W in sub-tables a – b. Sub-tables repeat the content explained in Table 13-1-a through Table 13-1-e.

LOGISTICS TABLES

Tables 1 through 3

Table 1
Mooring Stations and Trap Depths

Phase 1: Periods 1 to 13, April 3, 1989 to Sept. 26, 1989

Phase 2: Periods 14 to 27, Oct. 16, 1989 to April 16, 1990

(Hiatus: Sept. 26 1989 to Oct 16, 1989)

	34°N 21°W Station		48°N 21°W Station	
	Phase 1	**Phase 2**	**Phase 1**	**Phase 2**
Latitude	33°49'.3 N	33°48'.4 N	47°42'.9 N	47°43'.6 N
Longitude	21°00'.5 W	21°02'.2 W	20°52'.5 W	20°51'.5 W
Bottom Depth *	5,261 m	5,083 m	4,418 m	4,451 m
1 Km	1,070 m	1,248 m	1,018 m	1,202 m
2 Km	2,067 m	1,894 m	2,018 m	2,200 m
0.7 Km a.b.**	4,564 m	4,391 m	3,718 m	3,749 m
Deployed by	R/V Atlantis II	R/V Endeavor	R/V Atlantis II	R/V Endeavor
Recovered by	R/V Endeavor	RRV Darwin	R/V Endeavor	RRV Darwin

* Depths are all corrected values
** a.b. = above bottom

Table 2

Synchronized Open/Close Schedule for All Traps at the 34°N and 48°N, 21°W Stations

Period	Mid Date		Open/Close Date		Days Open	Elapsed Days
	JD*	CD*	JD*	CD*		
1	**96**	04/06/89	93	04/03/89	5	5
2	**105**	04/15/89	98	04/08/89	14	19
3	**119**	04/29/89	112	04/22/89	14	33
4	**133**	05/13/89	126	05/06/89	14	47
5	**148**	05/29/89	140	05/20/89	17	64
6	**164**	06/13/89	157	06/06/89	14	78
7	**178**	06/27/89	171	06/20/89	14	92
8	**192**	07/11/89	185	07/04/89	14	106
9	**206**	07/25/89	199	07/18/89	14	120
10	**220**	08/08/89	213	08/01/89	14	134
11	**234**	08/22/89	226	08/15/89	14	148
12	**248**	09/05/89	241	08/29/89	14	162
13	**262**	09/19/89	255	09/12/89	14	176
14	**279**	10/06/89	269	09/26/89	20 (hiatus)	196
15	**296**	10/23/89	289	10/16/89	14	210
16	**310**	11/06/89	303	10/30/89	14	224
17	**324**	11/20/89	317	11/13/89	14	238
18	**338**	12/04/89	331	11/27/89	14	252
19	**352**	12/18/89	345	12/11/89	14	266
20	**1**	01/01/90	359	21/25/89	14	280
21	**15**	01/15/90	8	01/08/90	14	294
22	**29**	01/29/90	22	01/22/90	14	308
23	**43**	02/12/90	36	02/05/90	14	322
24	**57**	02/26/90	50	02/19/90	14	336
25	**71**	03/12/90	64	03/05/90	14	350
26	**85**	03/26/90	78	03/19/90	14	364
27	**99**	04/09/90	92	04/02/90	14	378

*CD = Calendar Date; JD = Julian Date

Table 3

Specifications of Time-Series Sediment Trap (PARFLUX Mark 7G-13)

DIMENSIONS	
Height	152 cm
Diameter	91 cm
Approx. vertical surface area	0.66 m^2
WEIGHT (WITHOUT BRIDLES)	
In air with empty bottles	70 kg
In air with sample, water	75 kg
In water	35 kg
APERTURE/FUNNEL	
Aperture area	0.5 m^2
Aperture diameter	80 cm
Baffle material	Polycarbonate, 1/64"-thick wall
Approx. no. of baffle cells	368
Baffle cell diameter	25 mm
Aspect ratio of a cell (h/d)	2.5
Included cone-angle	42°
Bottom diameter (ID)	3.2 cm
ROTARY SAMPLER ASSEMBLY	
No. of sampling bottles	13
Standard container volume	250 ml
Rotary disk diameter	50 cm
Type of driving motor	Electronic stepping motor
Drive train	Direct gear train
Drive torque at the 2nd spur	30 kg/cm
Time to shift a bottle	31 sec.
TIMER/LOGGER	
Hardware	McLane ITC 1.6
Standard software	ITC Op. Prog. v 2.0
BATTERY	
Primary battery	McLane A14-1000 (21V)
Memory back-up	9 V alkaline battery
FRAME	
Material	Titanium unalloy, Ti - 45A/G-2
Structure	Weldment
Bridle configuration	3 and 3 in line, 1/2" insulated eye

PREPARATION TABLES

Tables 4 through 6

Table 4

Location, depth and nutrient concentration (μg-at kg^{-1}) in Initial Bottle Water

Sediment Trap Station	Deploy-ment Number	Sediment Trap Depth (m)	Locations and Depths of Initial Water Collection Sites				NO_3	NO_2	NH_4	TN	PO_4	TP	SiO_2	*Formalin %*	***Sodium Borate %*
34°N	01	1070	33°49.3'N	21°00'W	(5261)*	1000	13.0	6	0.3	18.0	0.86	1.1	7.2	3.0	0.1
		2067	"	"	"	3492	21.7	0	0.3	35.1	1.51	1.7	45.6	3.0	0.1
		4564	"	"	"	4092	21.7	0	0.3	35.7	1.51	1.9	51.3	3.0	0.1
48°N	01	1018	33°49.3'N	21°00'W	(5261)	1000	13.0	6	0.3	18.0	0.86	1.1	7.2	3.0	0.1
		2018	"	"	"	3492	21.7	0	0.3	35.1	1.51	1.7	45.6	3.0	0.1
		3718	"	"	"	4092	21.7	0	0.3	35.7	1.51	1.9	51.3	3.0	0.1
34°N	02	1248	47°43.2'N	20°52.2°W	(4375)	1200	7.77	02	0	12.3	1.35	1.42	14.3	3.0	0.1
		1894	"	"	"	1200	7.77	02	0	12.3	1.35	1.42	14.3	3.0	0.1
		4391	"	"	"	1200	7.77	02	0	12.3	1.35	1.42	14.3	3.0	0.1
48°N	02	1202	59°58.4"N	19°58.9'W	(2745)	1200	8.16	0.03	0.23	24.1	1.20	1.28	11.8	3.0	0.1
		2202	"	"	"	1200	8.16	0.03	0.23	24.1	1.20	1.28	11.8	3.0	0.1
		3749	"	"	"	1200	8.16	0.03	0.23	24.1	1.20	1.28	11.8	3.0	0.1

* Corrected depth of the site where initial bottle waters were collected

** Buffer

Table 5 - a

34°N Station, Concentration of Dissolved Nutrients (μg-at kg^{-1})

Sediment Trap Depth (m)	Deployment	Initial Bottle Water	Water Column	50% Exchange	Range When Recovered
PHOSPHORUS					
1070	01	0.86	0.78	0.82	5 — 347
1248	02	1.35	0.78	1.07	9 — 47
2067	01	1.51	1.09	1.30	5 — 29
1894	02	1.35	1.09	1.22	5 — 26
4564	01	1.51	1.41	1.28	3 — 88
4391	02	1.35	1.41	1.38	3 — 12
SILICA					
1070	01	7.2	10.9	9.05	26 - 901
1248	02	12.6	10.9	11.75	79 - 576
2067	01	45.6	17.0	31.3	121 - 735
1894	02	12.6	17.0	14.8	54 - 508
4564	01	51.3	47.7	49.5	108 - 755
4391	02	12.6	47.7	30.2	96 - 359
NITROGEN					
1070	01	18.0	18.6	18.3	5.1 - 8.3
1248	02	11.9	18.6	15.3	15 - 25
2067	01	35.1	19.0	27.1	5.0 - 11
1894	02	13.0	19.0	16.0	14 - 27
4564	01	35.7	22.9	29.3	9 - 11
4391	02	12.3	22.9	17.6	18 - 26

Table 5 - b

48°N Station, Concentration of Dissolved Nutrients (μg-at kg^{-1})

Sediment Trap Depth (m)	Deployment	Initial Bottle Water	Water Column	50% Exchange	Range When Recovered
PHOSPHORUS					
1818	01	0.86	1.11	0.99	19 – 26
1262	02	1.27	1.11	1.19	11 – 175
2018	01	1.51	1.13	1.32	7 – 49
2202	02	1.27	1.13	1.20	11 – 91
3718	01	1.51	1.42	1.47	4 – 17
3749	02	1.27	1.42	0.90	3 – 91
SILICA					
1818	01	7.2	11.2	9.20	162 – 887
1262	02	12.8	11.2	12.0	89 – 409
2018	01	45.6	12.0	28.8	217 – 875
2202	02	12.8	12.0	12.4	125 – 305
3718	01	53.3	38.6	46.0	181 – 797
3749	02	12.8	38.6	25.7	125 – 407
NITROGEN					
1818	01	18.0	18.1	18.1	6.1 – 8.6
1262	02	24.1	18.1	21.1	17 – 25
2018	01	35.1	17.6	26.3	8 – 42
2202	02	33.7	17.6	25.7	14 – 21
3718	01	35.7	21.6	28.7	9 – 16
3749	02	12.1	21.6	16.9	16 – 27

Table 6

Interim Times to Deliver "Normalized Times"

		34°N 21°W				48°N 21°N			
	Km	Pre–	Bloom	Post–	Total	Pre–	Bloom	Post–	Total
Sample Collection Time	1	70	117	129▼	316	154	106	98	358
	2	84	145	129	358	42†	92	84	218
	D	98	148	84	330	168	106	84	358
Percent: (Sample Collection	1	67.3	80.7	0▼	83.6	88.5	100	100	94.7
Time/Actual Collect. Time)	2	80.8	100	100	94.7	25.0†	86.8	80.8	57.7
	D	100	100	63.6	87.3	100	100	80.8	94.7
Actual Collection Times	1	104	145	129	378	174	106	98	378
	2	104	145	129	378	168	106	104	378
	D	98	145	132	378	168	106	104	378
Percent: (Actual Collection	1	27.5	38.4	34.1	100	46.1	28.0	25.9	100
Time/Total Actual Collect.	2	27.5	38.4	34.1	100	44.5	28.0	27.5	100
Time)	D	25.9	34.9	39.2	100	44.5	28.0	27.5	100
Normalized Collection Times	1	100	140	128	365	168	102	95	365
	2	100	140	125	365	163	102	100	365
	D	98	143	127	365	163	102	100	165
Normalized Collection Time Used in Report		100	140	125	365	163	102	100	365

▼ Partial clogging of the bottle mouth due to a fish head that restricted collection during this period.

† Total clogging of the bottle mouth due to a fish head that prevented collection in 9 of 12 samples in this period. Calculations are based on three samples which represent 25% of the episode.

SUMMARY TABLES

Tables 7 through 12

Table 7

		Km	34°N 21°W Pre–	Bloom	Post–	Annual	48°N 21°N Pre–	Bloom	Post–	Annual
Episodes *	Days		100	140	125	365	163	102	100	365
	Percent		27.5	38.4	34.1	100	45.5	28.0	27.5	100
Flux per episode (ep)**	g m^{-2} ep^{-1}	1	2.2	16.3	0.3▼	19.4	3.9†	12.4	4.4	19.9
		2	2.8	14.2	5.3	22.4	4.8	14.4	7.7	26.9
		D	3.2	13.1	4.9	21.2	5.6	12.7	7.8	26.2
Proportion (%) in a year		1	11.5	87.0	1.6	100	20.2	56.8	23.1	100
		2	12.6	63.5	23.9	100	12.9	53.4	28.7	100
		D	15.1	61.8	23.1	100	21.5	48.6	29.9	100
Average Flux	mg m^{-2} d^{-1}	1	22.3	121	2.5	79.4	24.0	121	44.2	54.5
		2	28.3	101	42.8	60.5	29.6	141	77.4	71.5
		D	31.0	93.3	39.1	57.3	34.5	124	78.2	69.9

* The boundaries of each episode were first defined at 1 km; then these boundaries were shifted to one period later for the 2 km depth; and then again to one more period later for the 0.7-km-a.b. depth.

** The average flux of the collected data for a given episode was used as fill-in data for missing periods and/or hiatuses for that episode.

▼ Partial clogging of the sediment-trap aperture due to a fish head that restricted collection during this period.

† Total clogging of the sediment-trap aperture due to a fish head that prevented collection in 9 of 12 samples in this period. Calculations are based on three samples which represent 25% of the time.

Table 8

Fluxes and Proportions (%) of Principal Sedimentary Components per Episode at 34°N 21°W

		Km	Pre-	Bloom	Post-	Annual
Total Flux	g m^{-2}	1	2.2	16.9	0.31	19.4
		2	2.8	14.2	5.3	22.4
		D*	3.2	13.1	4.9	21.2
	%	1	11.5	87.0	1.6	100
		2	12.6	63.5	23.9	100
		D	15.1	61.8	23.1	100
$CaCO_3$	g m^{-2}	1	1.6	11.4	0.15	13.1
		2	1.7	8.6	3.5	13.8
		D	1.9	7.9	3.1	12.9
	%	1	8.1	58.7	0.75	67.6
		2	7.8	38.4	15.6	61.8
		D	8.9	37.3	14.6	60.8
Opal	g m^{-2}	1	0.18	1.37	0.08	1.64
		2	0.24	1.21	0.60	2.04
		D	0.28	1.21	0.51	2.00
	%	1	0.95	7.07	0.39	8.41
		2	1.06	5.40	2.68	9.14
		D	1.34	5.71	2.39	9.44
POC	g m^{-2}	1	0.097	0.87	0.04	1.00
		2	0.11	0.68	0.23	1.03
		D	0.11	0.60	0.16	0.86
	%	1	0.50	4.46	0.19	5.15
		2	0.51	3.03	1.05	4.59
		D	0.53	2.82	0.74	4.09
PON	mg m^{-2}	1	14.9	150	5.98	172
		2	16.3	103	29.7	148
		D	19.0	81.4	14.0	114
	%	1	0.08	0.78	0.03	0.88
		2	0.07	0.46	0.13	0.66
		D	0.07	0.38	0.09	0.54
POP	mg m^{-2}	1	4.2	55.1	—	59.3
		2	3.0	11.8	5.9	20.7
		D	1.9	9.9	2.7	14.5
	%	1	0.02	0.28	—	0.30
		2	0.01	0.05	0.03	0.09
		D	0.01	0.05	0.01	0.07

*D: Trap deployed at the deepest level: 0.7 km above bottom

Table 9

Fluxes and Proportions (%) of Principal Sedimentary Components per Episode at 48°N 21°W

		Km	Pre–	Bloom	Post–	Annual
Total Flux	g m^{-2}	1	3.9	12.4	4.4	19.9
		2	4.8	14.4	7.5	26.9
		D*	5.6	12.7	7.8	26.2
	%	1	20.3	56.7	23.1	100
		2	17.9	53.4	28.7	100
		D	21.5	48.6	29.9	100
$CaCO_3$	g m^{-2}	1	2.4	6.9	2.2	11.0
		2	2.9	7.7	4.3	14.9
		D	3.5	7.6	4.3	15.4
	%	1	12.2	31.8	11.3	55.3
		2	10.6	28.6	16.1	55.3
		D	13.2	29.2	16.5	58.9
Opal	g m^{-2}	1	0.53	2.57	0.61	3.53
		2	0.76	3.73	1.41	5.91
		D	0.92	2.89	1.80	5.61
	%	1	2.76	11.8	3.21	17.8
		2	2.84	13.8	5.25	21.9
		D	3.52	11.0	6.89	21.4
POC	g m^{-2}	1	0.26	0.71	0.55	1.48
		2	0.28	0.66	0.44	1.38
		D	0.22	0.49	0.29	1.00
	%	1	1.33	3.25	2.86	7.43
		2	1.02	2.46	1.65	5.13
		D	0.85	1.88	1.10	3.83
PON	mg m^{-2}	1	37.9	119	68.5	218
		2	39.5	105	60.4	205
		D	29.6	73.7	37.5	140
	%	1	0.20	0.55	0.36	1.10
		2	0.15	0.39	0.22	0.76
		D	0.11	0.28	0.14	0.54
POP	mg m^{-2}	1	13.5	17.9	9.4	40
		2	11.6	12.6	9.4	33.4
		D	6.5	7.2	3.6	17.2
	%	1	0.07	0.08	0.05	0.20
		2	0.04	0.05	0.04	0.12
		D	0.02	0.03	0.01	0.07

*D: Trap deployed at the deepest level: 0.7 km above bottom

Table 10

Molar Ratios between Critical Biogeochemical Elements During Each Episode at 34°N 21W

	Km	Pre–	Bloom	Post–	Annual
Ca_{carb}/Si	1	5.11	4.99	1.17	4.78
	2	4.41	4.28	3.51	4.06
	D	3.98	3.93	3.67	3.89
C_{org}/C_{inorg}	1	0.51	0.63	2.14	0.64
	2	0.55	0.66	0.56	0.62
	D	0.50	0.63	0.42	0.57
C/N	1	7.58	6.71	7.33	6.80
	2	8.21	7.71	9.21	8.06
	D	9.31	8.54	9.64	8.75
C/P	1	58	40	—	47
	2	99	148	102	128
	D	153	154	151	154
N/P	1	7.8	6.1	—	6.8
	2	12.2	19.3	11.1	16.0
	D	16.5	18.1	15.7	17.6
C_{org}/Si	1	2.63	3.16	2.49	3.07
	2	2.43	2.81	1.96	2.52
	D	1.97	2.47	1.56	2.23

Table 11

Molar Ratios between Critical Biogeochemical Elements During Each Episode at 48°N 21°W

	Km	Pre–	Bloom	Post–	Annual
Ca_{carb}/Si	1	2.65	1.62	2.11	1.84
	2	2.25	1.24	1.85	1.43
	D	2.25	1.59	1.44	1.66
C_{org}/C_{inorg}	1	0.91	0.85	2.11	1.09
	2	0.80	0.72	0.85	0.77
	D	0.54	0.54	0.55	0.54
C/N	1	7.91	6.95	9.32	7.80
	2	8.15	7.33	8.57	7.79
	D	8.74	7.79	8.95	8.26
C/P	1	49	101	150	96
	2	63	136	121	120
	D	89	177	209	148
N/P	1	6.2	14.7	16.1	12.4
	2	7.7	18.5	14.1	15.5
	D	10.1	22.7	23.3	17.9
C_{org}/Si	1	2.41	1.38	4.46	2.01
	2	1.81	0.89	1.57	1.10
	D	1.21	0.85	0.80	0.90

Table 12

Redfield Ratio

C : N : P

106 : 16 : 1

	34°N			48°N		
Pre-bloom	C	N	P	C	N	P
1 km	53	8	1	49	6	1
2 km	99	12	1	63	8	1
D	153	17	1	89	10	1
Bloom						
1 km	40	6	1	101	15	1
2 km	148	19	1	136	19	1
D	154	18	1	177	23	1
Post						
1 km	—	—	—	150	16	1
2 km	102	11	1	121	14	1
D	151	16	1	209	23	1
Annual						
1 km	47	7	1	96	12	1
2 km	128	16	1	120	16	1
D	154	18	1	148	18	1

TABLES GIVING FLUXES PER PERIOD

Tables 13 and 14

Table 13 - 1 - a

Fluxes of Particles by Size Fractions at 34°N 21°W, 1071 m and 1248 m; mg m^{-2} day^{-1}

Period	Mid JD	Total	>1mm	<1mm	>1mm (%)	<1mm (%)
1	96	35.1	0	35.1	0	100
2	105	142	6.96	135	4.90	95.1
3*	119	12.6	0	12.6	0	100
4*	133	4.27	0	4.27	0	100
5*	148	1.39	0	1.39	0	100
6*	164	0.921	0	0.921	0	100
7*	178	1.50	0	1.50	0	100
8*	192	0.0617	0	0.0617	0	100
9*	206	0.0856	0	0.0856	0	100
10*	220	11.4	0	11.4	0	100
11*	234	2.54	0	2.54	0	100
12*	248	0.203	0	0.203	0	100
13*	262	3.10	0	3.10	0	100
14	279	— (Hiatus) —				
15	296	21.0	0	21.0	0	100
16	310	18.2	0	18.2	0	100
17	324	19.1	0	19.1	0	100
18	338	32.4	0	32.3	0	100
19	352	20.6	0	20.6	0	100
20	1	50.4	0	50.4	0	100
21	15	88.3	4.37	83.9	4.95	95.0
22	29	154	11.7	142	7.60	92.4
23	43	114	7.48	106	6.58	93.4
24	57	95.2	3.00	92.2	3.15	96.8
25	71	219	32.4	187	14.8	85.2
26	85	133	11.7	122	8.76	91.2
27	99	(Total clogging of the sample bottle due to a fish head)				

* Collection was limited because the sample bottle was partially clogged by a fish head

Table 13 - 1 - b

Fluxes of Ca, C_{inorg}, C_{org} and N_{org} at 34°N 21°W, 1071 m and 1248 m

Period	Mid JD	$CaCO_3$	Ca in $CaCO_3$	C inorg	N org	C org	$CaCO_3$	Ca in $CaCO_3$	C inorg	N org	C org
		mg m^{-2} day^{-1}					percent				
1	96	25.7	10.3	3.09	0.554	2.88	73.3	29.3	8.80	1.58	8.21
2	105	77.6	31.1	9.31	1.15	7.39	54.6	21.9	6.55	0.81	5.20
3*	119	1.60	0.639	0.192	0.489	2.85	12.7	5.09	1.52	3.89	22.7
4*	133	1.97	0.789	0.237	0.0648	0.458	46.2	18.5	5.54	1.52	10.7
5*	148	0.675	0.270	0.0810	0.0376	0.213	48.7	19.5	5.84	2.71	15.4
6*	164	0.411	0.165	0.0494	0.0278	0.139	44.7	17.9	5.36	3.02	15.1
7*	178	0.343	0.137	0.0412	0.0558	0.293	22.8	9.13	2.74	3.71	19.5
8*	192	0	0	0	0	0	0	0	0	0	0
9*	206	0	0	0	0	0	0	0	0	0	0
10*	220	6.35	2.544	0.762	0.197	1.31	55.7	22.3	6.68	1.73	11.5
11*	234	0.911	0.365	0.109	0.0492	0.316	35.9	14.4	4.31	1.94	12.5
12*	248	0	0	0	0	0	0	0	0	0	0
13*	262	0.824	0.330	0.0989	0.0654	0.461	26.6	10.7	3.19	2.11	14.9
14	279	— (Hiatus) —									
15	296	15.2	6.11	1.83	0.141	0.918	72.5	29.0	8.70	0.670	4.36
16	310	12.3	4.93	1.48	0.133	0.772	67.6	27.1	8.11	0.730	4.24
17	324	13.5	5.39	1.61	0.136	0.901	70.3	28.1	8.44	0.710	4.71
18	338	23.5	9.39	2.81	0.175	1.17	72.5	29.0	8.70	0.540	3.63
19	352	14.2	5.67	1.70	0.160	1.08	68.8	27.5	8.26	0.780	5.24
20	1	34.4	13.8	4.13	0.393	2.54	68.4	27.4	8.21	0.780	5.05
21	15	65.1	26.1	7.81	0.565	3.89	73.7	29.5	8.84	0.640	4.41
22	29	119	47.8	14.3	0.924	5.90	77.5	31.0	9.30	0.600	3.83
23	43	88.6	35.5	10.6	0.727	4.35	78.0	31.2	9.36	0.640	3.83
24	57	68.8	27.6	8.26	0.990	3.66	72.3	28.9	8.68	1.04	3.84
25	71	148	59.4	17.8	2.24	12.7	67.7	27.1	8.12	1.02	5.79
26	85	69.8	28.0	8.38	1.81	10.3	52.4	21.0	6.29	1.36	7.71
27	99	— (Total clogging of the sample bottle due to a fish-head) —									

* Collection was limited because the sample bottle was partially clogged by a fish head

Table 13 - 1 - c

Opal Fluxes at 34°N 21°W, 1071 m and 1248 m (mg m^{-2} day^{-1})

Period	Mid JD	SiO_2 opal	SiO_2 part	SiO_2 diss	Si in opal	SiO_2 opal	SiO_2 part	SiO_2 diss	Si in opal
		mg m^{-2} day^{-1}				percent			
1	96	3.29	2.32	0.970	1.55	9.38	6.61	2.77	4.38
2	105	18.5	16.6	1.88	8.62	13.0	11.7	1.32	6.06
3*	119	3.35	2.29	1.06	1.57	26.6	18.2	8.37	12.4
4*	133	1.25	0.866	0.379	0.585	29.2	20.3	8.89	13.6
5*	148	0.294	0.168	0.120	0.137	20.7	12.1	8.64	9.68
6*	164	0.314	0.217	0.088	0.146	33.2	23.6	9.63	15.5
7*	178	0.295	0.228	0.059	0.138	19.1	15.2	3.93	8.92
8*	192	0.079	0.014	0.057	0.037	115	22.2	92.4	53.5
9*	206	0.043	0	0.034	0.020	41.1	1.47	39.6	19.2
10*	220	2.59	1.82	0.756	1.21	22.6	16.0	6.63	10.6
11*	234	0.579	0.386	0.185	0.270	22.5	15.2	7.31	10.5
12*	248	0.065	0.025	0.032	0.030	27.9	12.3	15.6	13.0
13*	262	0.707	0.499	0.200	0.330	22.6	16.1	6.46	10.5
14	279			— (Hiatus) —					
15	296	1.62	1.42	0.192	0.758	7.67	6.76	0.911	3.58
16	310	1.45	1.28	0.158	0.677	7.92	7.05	0.869	3.70
17	324	1.92	1.76	0.143	0.894	9.97	9.22	0.749	4.66
18	338	2.66	2.28	0.372	1.24	8.19	7.04	1.15	3.83
19	352	1.59	1.44	0.141	0.744	7.71	7.02	0.687	3.60
20	1	4.20	3.70	0.488	1.96	8.32	7.35	0.970	3.89
21	15	6.39	5.75	0.634	2.98	7.23	6.51	0.718	3.38
22	29	12.6	11.4	1.19	5.88	8.17	7.40	0.772	3.82
23	43	8.21	7.27	0.930	3.83	7.22	6.40	0.819	3.37
24	57	7.32	6.68	0.627	3.42	7.68	7.02	0.659	3.59
25	71	16.0	15.2	0.751	7.45	7.27	6.93	0.343	3.40
26	85	7.75	7.13	0.615	3.62	5.81	5.35	0.462	2.72
27	99				(Total clogging of the sample bottle due to a fish head)				

* Collection was limited because the sample bottle was partially clogged by a fish head

Table 13 - 1 - d

Phosphorus Fluxes at 34°N 21°W, 1071 m and 1248 m

Period	Mid JD	P total	P part	P diss	P total	P part	P diss
		$\mu g\ m^{-2}\ day^{-1}$			ppm		
1	96	3290	0	3291	9383	0	9383
2	105	2830	2488	342	1991	1750	240
3*	119	—	—	409	—	—	3250
4*	133	—	—	3770	—	—	88300
5*	148	—	—	791	—	—	57000
6*	164	—	—	465	—	—	50600
7*	178	—	—	443	—	—	29500
8*	192	—	—	486	—	—	787000
9*	206	—	—	191	—	—	224000
10*	220	—	—	187	—	—	1650
11*	234	—	—	104	—	—	4110
12*	248	—	—	43.1	—	—	21200
13*	262	—	—	64.9	—	—	2090
14	279	—	— (Hiatus) —				
15	296	702	202	497	3330	962	2370
16	310	236	132	101	1290	728	569
17	324	253	141	109	1320	737	586
18	338	325	231	91.5	1000	714	290
19	352	616	185	428	2990	902	2090
20	1	446	339	104	886	675	211
21	15	872	708	161	987	802	185
22	29	1100	957	140	714	621	92.7
23	43	1000	820	178	880	721	158
24	57	955	686	267	1000	720	282
25	71	2050	1887	163	936	861	75.6
26	85	22500	2080	20378	16800	1561	15200
27	99			(Total clogging of the sample bottle due to a fish-head)			

* Collection was limited because the sample bottle was partially clogged by a fish head

Table 13 - 1 - e

34°N 21°W, 1071m and 1248 m
Ratios (Molar) of critical biogenic elements

Period	Mid JD	Ca/Si	C/N	C/P	N/P	C_{org}/C_{inorg}	C_{org}/Si
1	96	4.66	6.06	22.6	3.73	0.934	4.35
2	105	2.52	7.49	67.4	9.00	0.794	2.01
3*	119	0.286	6.81	—	—	14.9	4.26
4*	133	0.944	8.23	—	—	1.94	1.83
5*	148	1.38	6.61	—	—	2.63	3.63
6*	164	0.787	5.84	—	—	2.82	2.22
7*	178	0.697	6.12	—	—	7.11	4.97
8*	192	—	—	—	—	—	—
9*	206	—	—	—	—	—	—
10*	220	1.47	7.72	—	—	1.71	2.53
11*	234	0.944	7.49	—	—	2.89	2.73
12*	248	0.000	—	—	—	—	—
13*	262	0.700	8.23	—	—	4.66	3.27
14	279			— (Hiatus) —			
15	296	5.65	7.59	33.8	4.46	0.501	2.83
16	310	5.10	6.78	85.2	12.6	0.523	2.67
17	324	4.22	7.47	92.6	11.9	0.558	2.36
18	338	5.38	7.84	93.9	11.9	0.417	2.21
19	352	5.33	7.84	45.2	5.78	0.635	3.39
20	1	4.92	7.55	147	19.6	0.615	3.03
21	15	6.11	8.04	115	14.4	0.499	3.05
22	29	5.69	7.45	139	18.6	0.412	2.35
23	43	6.48	6.98	112	16.1	0.409	2.65
24	57	5.64	4.31	99.0	23.0	0.443	2.50
25	71	5.58	6.62	160	24.1	0.713	3.99
26	85	5.41	6.61	11.8	1.78	1.23	6.64
27	99		(Total clogging of the sample bottle due to a fish-head)				

* Collection was limited because the sample bottle was partially clogged by a fish head

Table 13 - 2 - a

Fluxes of Particles by Size Fractions at 34°N 21°W, 2067 m and 1894 m ; mg m^{-2} day^{-1}

Period	Mid JD	Total	>1mm	<1mm	>1mm (%)	<1mm (%)
1	96	20.2	0	20.2	0	100
2	105	106	0	106	0	100
3	119	117	0	117	0	100
4	133	91.7	0	91.7	0	100
5	148	61.9	0	61.9	0	100
6	164	40.9	0	40.9	0	100
7	178	40.5	0	40.6	0	100
8	192	45.1	0	45.1	0	100
9	206	46.4	0	46.4	0	100
10	220	35.4	0	35.4	0	100
11	234	37.4	0	37.4	0	100
12	248	33.7	0	33.7	0	100
13	262	39.3	0	39.3	0	100
14	279	— (Hiatus) —				
15	296	20.2	0	20.2	0	100
16	310	24.8	0	24.8	0	100
17	324	24.2	0	24.2	0	100
18	338	24.9	0	24.9	0	100
19	352	27.6	0	27.6	0	100
20	1	47.9	0	47.9	0	100
21	15	73.8	0	73.8	0	100
22	29	137	11.8	125	8.65	91.4
23	43	171	20.0	151	11.7	88.3
24	57	84.9	3.65	81.2	4.31	95.7
25	71	141	12.9	128	9.11	90.9
26	85	190	23.0	167	12.1	87.9
27	99	66.5	7.02	59.5	10.6	89.4

Table 13 - 2 - b

Fluxes of Ca, C_{inorg}, C_{org} and N_{org}
at 34°N 21°W, 2067 m and 1894 m

Period	Mid JD	$CaCO_3$	Ca in $CaCO_3$	C inorg	N org	C org	$CaCO_3$	Ca in $CaCO_3$	C inorg	N org	C org
		mg m^{-2} day^{-1}					percent				
1	96	14.0	5.59	1.68	0.133	0.840	69.2	27.7	8.30	0.660	4.16
2	105	63.5	25.4	7.62	0.614	4.70	60.0	24.0	7.20	0.580	4.44
3	119	66.7	26.7	8.00	0.667	5.02	57.0	22.8	6.84	0.570	4.29
4	133	53.4	21.4	6.41	0.587	4.35	58.2	23.3	6.98	0.640	4.74
5	148	41.5	16.6	4.98	0.297	2.26	67.0	26.8	8.04	0.480	3.65
6	164	27.5	11.0	3.30	0.217	1.54	67.1	26.9	8.05	0.530	3.77
7	178	27.0	10.8	3.25	0.215	1.69	66.7	26.7	8.00	0.530	4.17
8	192	28.1	11.2	3.37	0.293	2.13	62.3	24.9	7.48	0.650	4.72
9	206	30.1	12.0	3.61	0.250	2.08	64.8	25.9	7.78	0.540	4.49
10	220	22.8	9.11	2.73	0.212	1.88	64.3	25.7	7.72	0.600	5.30
11	234	24.1	9.63	2.89	0.213	1.83	64.3	25.7	7.72	0.570	4.89
12	248	21.9	8.79	2.63	0.199	1.61	65.2	26.1	7.82	0.590	4.79
13	262	26.3	10.5	3.15	0.228	1.78	66.8	26.7	8.02	0.580	4.53
14	279				— (Hiatus) —						
15	296	13.3	5.33	1.60	0.111	0.779	65.8	26.3	7.90	0.550	3.85
16	310	16.1	6.43	1.93	0.136	0.990	64.9	26.0	7.79	0.550	4.00
17	324	15.4	6.18	1.85	0.153	1.08	63.7	25.5	7.64	0.630	4.46
18	338	15.6	6.25	1.87	0.129	0.942	62.8	25.1	7.54	0.520	3.79
19	352	18.8	7.52	2.25	0.149	1.04	68.1	27.3	8.17	0.540	3.76
20	1	25.1	10.0	3.01	0.302	2.07	52.3	20.9	6.28	0.630	4.31
21	15	44.7	17.9	5.36	0.443	3.30	60.5	24.2	7.26	0.600	4.47
22	29	102	40.8	12.2	0.698	5.33	74.4	29.8	8.93	0.510	3.89
23	43	130	52.2	15.6	0.923	6.50	76.2	30.5	9.14	0.540	3.80
24	57	48.9	19.6	5.87	0.594	3.73	57.6	23.1	6.91	0.700	4.40
25	71	93.3	37.4	11.2	1.31	8.07	66.1	26.5	7.93	0.930	5.72
26	85	105.	42.0	12.6	1.94	11.6	55.2	22.1	6.62	1.02	6.10
27	99	27.6	11.1	3.31	0.419	2.43	41.5	16.6	4.98	0.630	3.65

Table 13 - 2 - c

Opal Fluxes at 34°N 21°W, 2067 m and 1894 m

Period	Mid JD	SiO_2 opal	SiO_2 part	SiO_2 diss	Si in opal	SiO_2 opal	SiO_2 part	SiO_2 diss	Si in opal
		mg m^{-2} day^{-1}				percent			
1	96	2.04	1.41	0.652	0.956	10.1	7.01	3.10	4.72
2	105	10.6	9.18	1.51	4.99	10.1	8.67	1.43	4.72
3	119	15.7	14.4	1.34	7.35	13.5	12.3	1.15	6.78
4	133	12.9	11.6	1.32	6.05	14.1	12.7	1.44	6.59
5	148	7.15	6.25	0.945	3.36	11.6	10.1	1.53	5.43
6	164	4.64	3.87	0.770	2.17	11.3	9.45	1.88	5.29
7	178	4.96	4.29	0.667	2.32	12.2	10.6	1.64	5.71
8	192	5.33	4.69	0.638	2.49	11.8	10.4	1.42	5.52
9	206	5.12	4.62	0.490	2.39	11.0	9.97	1.01	5.15
10	220	4.06	3.67	0.389	1.89	11.5	10.4	1.10	5.35
11	234	3.62	3.31	0.316	1.69	9.68	8.84	0.844	4.52
12	248	3.59	3.35	0.244	1.68	10.7	9.94	0.725	4.98
13	262	4.69	4.47	0.219	2.19	11.9	11.4	0.557	5.57
14	279	— (Haitus) —							
15	296	1.76	1.58	0.185	0.823	8.72	7.80	0.916	4.07
16	310	2.20	1.99	0.202	1.03	8.87	8.05	0.816	4.14
17	324	2.17	2.09	0.078	1.02	8.97	8.65	0.321	4.19
18	338	2.14	1.97	0.166	0.998	8.60	7.93	0.669	4.02
19	352	2.28	2.10	0.181	1.07	8.28	7.62	0.656	3.86
20	1	4.01	3.66	0.349	1.87	8.37	7.64	0.729	3.91
21	15	6.76	6.12	0.636	3.16	9.15	8.29	0.861	4.27
22	29	12.6	11.5	1.03	5.87	9.18	8.43	0.755	4.29
23	43	12.5	11.6	0.930	5.84	7.31	6.77	0.544	3.42
24	57	6.65	6.09	0.566	3.11	7.83	7.18	0.655	3.66
25	71	9.46	9.03	0.429	4.41	6.70	6.40	0.304	3.13
26	85	11.2	10.6	0.648	5.24	5.91	5.57	0.341	2.76
27	99	4.91	4.65	0.263	2.29	7.39	6.99	0.396	3.45

Table 13 - 2 - d

PhosphorusFluxes at 34°N 21°W, 2067 m and 1894 m

Period	Mid JD	P total	P part	P diss	P total	P part	P diss
		$\mu g\ m^{-2}\ day^{-1}$			ppm		
1	96	195	0	195	967	0	967
2	105	646	541	104	610	511	99.2
3	119	721	653	68.4	616	558	58.5
4	133	648	566	83.3	707	617	90.8
5	148	79.8	0	79.8	127	0	128
6	164	399	291	109	974	710	266
7	178	598	290	307	1470	716	758
8	192	1400	1291	112	3310	2864	251
9	206	369	272	96.9	794	587	208
10	220	296	255	41.2	833	720	116
11	234	551	398	153	1472	1064	411
12	248	283	216	67.0	837	641	199
13	262	379	333	46.7	962	847	118
14	279		— (Hiatus) —				
15	296	268	144	124	1320	710	616
16	310	282	188	94.8	1140	759	383
17	324	195	1 69	26.5	807	698	109
18	338	281	199	81.7	1130	802	378
19	352	423	212	211	1530	770	765
20	1	337	297	38.9	702	622	81.2
21	15	739	461	278	1000	625	376
22	29	969	830	139	707	606	101
23	43	150	1235	262	875	723	153
24	57	785	588	196	923	693	230
25	71	1320	1165	152	932	825	106
26	85	1850	1706	148	976	898	78.2
27	99	556	465	90.9	836	699	137

Table 13 - 2 - e

34°N 21°W, 2067m and 1894m
Ratios (Molar) of critical biogenic elements

Period	Mid JD	Ca/Si	C/N	C/P	N/P	C_{org}/C_{inorg}	C_{org}/Si
1	96	4.11	7.35	113	15.3	0.501	2.06
2	105	3.59	8.93	188	21.0	0.617	2.21
3	119	2.55	8.78	180	20.5	0.627	1.60
4	133	2.49	8.64	173	20.0	0.679	1.69
5	148	3.49	8.87	739	83.3	0.454	1.58
6	164	3.60	8.30	99.8	12.0	0.468	1.69
7	178	3.31	9.18	73.1	7.96	0.521	1.73
8	192	3.20	8.47	39.1	4.62	0.631	2.02
9	206	3.57	9.70	146	15.0	0.578	2.06
10	220	3.42	10.3	164	15.9	0.687	2.35
11	234	4.05	10.0	85.7	8.56	0.634	2.57
12	248	3.73	9.47	148	15.6	0.612	2.29
13	262	3.41	9.11	121	13.3	0.565	1.93
14	279		— (Hiatus) —				
15	296	4.54	8.17	75.1	9.20	0.488	2.21
16	310	4.40	8.48	90.7	10.7	0.514	2.26
17	324	4.27	8.26	143	17.4	0.584	2.49
18	338	4.39	8.50	86.8	10.2	0.503	2.21
19	352	4.94	8.12	63.3	7.80	0.460	2.28
20	1	3.76	7.98	159	19.9	0.687	2.58
21	15	3.97	8.69	115	13.3	0.616	2.45
22	29	4.87	8.90	142	16.0	0.436	2.13
23	43	6.26	8.21	112	13.6	0.416	2.61
24	57	4.42	7.33	123	16.8	0.637	2.84
25	71	5.92	7.17	158	22.1	0.721	4.30
26	85	5.61	6.98	161	23.1	0.921	5.19
27	99	3.38	6.76	113	16.7	0.733	2.50

Table 13 - 3 - a

Fluxes of Particles by Size Fractions at 34°N 21°W, 4564 m and 4391 m; mg m^{-2} day^{-1}

Period	Mid JD	Total	>1mm	<1mm	>1mm (%)	<1mm (%)
1	96	30.9	0	30.9	0	100
2	105	62.4	0	62.4	0	100
3	119	129	0	129	0	100
4	133	72.5	0	72.5	0	100
5	148	63.3	0	63.3	0	100
6	164	39.4	0	39.4	0	100
7	178	45.5	0	45.5	0	100
8	192	40.4	0	40.4	0	100
9*	206	—	—	—	—	—
10	220	38.0	0	38.0	0	100
11*	234	—	—	—	—	—
12	248	36.2	0	36.2	0	100
13	262	35.0	0	35.0	0	100
14	279		— (Hiatus) —			
15	296	26.2	0	26.2	0	100
16	310	28.7	0	28.7	0	100
17	324	29.5	0	29.5	0	100
18	338	25.1	0	25.1	0	100
19	352	24.4	0	24.3	0	100
20	1	32.9	0	32.9	0	100
21	15	57.6	0	57.6	0	100
22	29	77.6	2.44	75.1	3.14	96.9
23	43	139	7.42	132	5.33	94.7
24	57	81.4	3.47	78.0	4.27	95.7
25	71	95.8	10.0	85.8	10.5	89.5
26	85	165	33.0	132	20.0	80.0
27	99	75.7	8.80	66.9	11.6	88 4

* Samples destroyed in transit

Table 13 - 3 - b

Fluxes of Ca, C_{inorg}, C_{org} and N_{org} at 34°N 21°W, 4564 m and 4391 m

Period	Mid JD	$CaCO_3$	Ca in $CaCO_3$	C inorg	N org	C org	$CaCO_3$	Ca in $CaCO_3$	C inorg	N org	C org
		mg m^{-2} day^{-1}					percent				
1	96	19.4	7.76	2.33	0.133	1.07	62.8	25.1	7.54	0.430	3.46
2	105	38.0	15.2	4.56	0.268	2.22	60.8	24.3	7.30	0.430	3.55
3	119	81.6	32.7	9.79	0.634	4.89	63.0	25.2	7.56	0.490	3.78
4	133	46.2	18.5	5.55	0.355	2.78	63.8	25.5	7.66	0.490	3.83
5	148	40.6	16.3	4.88	0.397	2.41	64.2	25.7	7.70	0.470	3.81
6	164	24.5	9.81	2.94	0.134	1.06	62.2	24.9	7.46	0.340	2.69
7	178	29.5	11.8	3.54	0.173	1.38	64.9	26.0	7.79	0.380	3.04
8	192	26.1	10.4	3.13	0.158	1.29	64.5	25.8	7.74	0.390	3.19
9*	206	—	—	—	—	—	—	—	—	—	—
10	220	23.1	9.25	2.77	0.160	1.35	60.8	24.3	7.30	0.420	3.56
11*	234	—	—	—	—	—	—	—	—	—	—
12	248	22.8	9.14	2.74	0.163	1.41	63.0	25.2	7.56	0.450	3.89
13	262	22.3	8.93	2.68	0.126	1.05	63.8	25.5	7.66	0.360	3.00
14	279				— (Hiatus) —						
15	296	17.3	6.92	2.07	0.110	0.901	66.0	26.4	7.92	0.420	3.44
16	310	17.6	7.04	2.11	0.118	0.909	61.3	24.5	7.36	0.410	3.17
17	324	18.2	7.30	2.19	0.118	0.961	61.9	24.8	7.43	0.400	3.26
18	338	15.9	6.36	1.91	0.103	0.801	63.3	25.3	7.60	0.410	3.19
19	352	15.8	6.31	1.89	0.0974	0.801	64.7	25.9	7.76	0.400	3.29
20	1	20.3	8.14	2.44	0.141	1.12	61.8	24.7	7.42	0.430	3.41
21	15	26.3	10.5	3.16	0.294	2.33	45.7	18.3	5.48	0.510	4.05
22	29	37.5	15.0	4.51	0.372	2.89	48.4	19.4	5.81	0.480	3.72
23	43	80.6	32.3	9.67	0.724	5.62	57.9	23.2	6.95	0.520	4.04
24	57	58.9	23.6	7.07	0.432	3.26	72.3	28.9	8.68	0.530	4.00
25	71	64.1	25.7	7.69	0.805	5.57	66.9	26.8	8.03	0.840	5.81
26	85	91.4	36.6	11.0	1.66	11.0	55.5	22.2	6.66	1.01	6.69
27	99	41.9	16.8	5.03	0.484	3.43	55.4	22.2	6.65	0.640	4.53

* Samples destroyed in transit

Table 13 - 3 - c

Opal Fluxes at 34°N 21°W, 4564 m and 4391 m (mg m^{-2} day^{-1})

Period	Mid JD	SiO_2 opal	SiO_2 part	SiO_2 diss	Si in opal	SiO_2 opal	SiO_2 part	SiO_2 diss	Si in opal
		mg m^{-2} day^{-1}				percent			
1	96	2.91	2.53	0.377	1.36	9.44	8.19	1.25	4.40
2	105	5.96	4.94	1.02	2.78	9.55	7.91	1.64	4.46
3	119	17.2	15.7	1.49	8.03	13.3	12.1	1.15	6.20
4	133	9.31	8.25	1.06	4.35	12.9	11.4	1.46	6.00
5	148	7.41	6.69	0.723	3.46	11.7	10.6	1.14	5.47
6	164	4.19	3.68	0.507	1.95	10.6	9.34	1.29	4.96
7	178	4.78	4.39	0.396	2.23	10.5	9.64	0.870	4.91
8	192	4.14	3.80	0.337	1.93	10.2	9.41	0.833	4.78
9*	206	—	—	—	—	—	—	—	—
10	220	3.72	3.48	0.248	1.74	9.81	9.15	0.654	4.58
11*	234	—	—	—	—	—	—	—	—
12	248	3.81	3.65	0.160	1.78	10.5	10.1	0.442	4.92
13	262	3.64	3.52	0.124	1.70	10.4	10.1	0.355	4.87
14	279			— (Hiatus) —					
15	296	2.29	2.12	0.171	1.07	8.74	8.09	0.654	4.08
16	310	2.74	2.57	0.171	1.28	9.56	8.96	0.597	4.46
17	324	2.84	2.66	0.186	1.33	9.65	9.02	0.631	4.50
18	338	2.28	2.15	0.131	1.07	9.09	8.57	0.522	4.24
19	352	2.44	2.34	0.102	1.14	10.0	9.60	0.418	4.67
20	1	2.94	2.82	0.119	1.37	8.94	8.58	0.360	4.17
21	15	4.32	4.05	0.274	2.02	7.52	7.04	0.477	3.51
22	29	7.25	6.65	0.609	3.39	9.35	8.57	0.785	4.37
23	43	11.4	10.7	0.655	5.31	8.17	7.70	0.471	3.81
24	57	6.39	6.03	0.365	2.98	7.84	7.40	0.448	3.66
25	71	7.73	7.55	0.186	3.61	8.07	7.88	0.194	3.77
26	85	11.0	10.8	0.207	5.12	6.65	6.53	0.126	3.11
27	99	4.96	4.78	0.177	2.32	6.55	6.32	0.234	3.06

* Samples destroyed in transit

Table 13 - 3 - d

Phosphorus Fluxes at 34°N 21°W, 4564 m and 4391m

Period	Mid JD	P total	P part	P diss	P total	P part	P diss
		$\mu g\ m^{-2}\ day^{-1}$			ppm		
1	96	29.2	0	29.2	94.7	0	94.7
2	105	464	333	131	743	533	210
3	119	779	745	33.6	601	576	25.9
4	133	359	335	24.0	495	463	33.2
5	148	1200	418	781	1890	661	1230
6	164	205	186	18.7	520	473	47.5
7	178	227	192	34.9	498	422	76.7
8	192	204	185	18.7	504	458	46.3
9*	206	—	—	—	—	—	—
10	220	248	222	25.5	651	585	66.9
11*	234	—	—	—	—	—	—
12	248	197	181	16.0	542	499	44.1
13	262	192	176	16.0	550	504	45.7
14	279		— (Hiatus) —				
15	296	162	131	31.2	618	499	119
16	310	187	152	35.6	652	529	124
17	324	200	176	24.0	678	597	81.6
18	338	137	121	15.6	546	485	61.9
19	352	144	125	18.4	589	514	75.5
20	1	175	159	15.6	532	485	47.3
21	15	295	277	17.2	512	482	29.8
22	29	404	386	17.2	520	498	22.1
23	43	944	836	108	678	601	77.6
24	57	428	404	23.5	525	496	28.8
25	71	695	662	33.2	725	691	34.6
26	85	1320	1261	55.6	799	766	33.7
27	99	616	500	16.4	814	660	154

* Samples destroyed in transit

Table 13 - 3 - e

34°N 21°W, 4564 m and 4391 m
Ratios (Molar) of critical biogenic elements

Period	Mid JD	Ca/Si	C/N	C/P	N/P	C_{org}/C_{inorg}	C_{org}/Si
1	96	4.01	9.39	942	100	0.459	1.84
2	105	3.83	9.63	123	12.7	0.487	1.86
3	119	2.85	9.00	162	17.9	0.500	1.43
4	133	2.98	9.12	198	21.7	0.500	1.49
5	148	3.29	9.46	52	5.47	0.495	1.63
6	164	3.52	9.23	132	14.3	0.360	1.27
7	178	3.71	9.33	156	16.7	0.390	1.45
8	192	3.78	9.54	161	16.9	0.412	1.56
9*	206	—	—	—	—	—	—
10	220	3.73	9.89	140	14.1	0.488	1.82
11*	234	—	—	—	—	—	—
12	248	3.59	10.1	183	18.1	0.515	1.85
13	262	3.68	9.72	139	14.3	0.392	1.44
14	279		— (Hiatus) —				
15	296	4.54	9.55	142	14.8	0.434	1.97
16	310	3.86	9.02	124	13.7	0.431	1.66
17	324	3.86	9.51	122	12.9	0.439	1.69
18	338	4.19	9.08	148	16.3	0.420	1.76
19	352	3.89	9.59	142	14.8	0.424	1.65
20	1	4.16	9.25	163	17.6	0.460	1.91
21	15	3.66	9.26	202	21.8	0.739	2.70
22	29	3.11	9.04	183	20.3	0.641	1.99
23	43	4.26	9.06	153	16.9	0.582	2.48
24	57	5.54	8.80	195	22.2	0.461	2.55
25	71	4.98	8.07	206	25.5	0.724	3.61
26	85	5.01	7.73	215	27.9	1.00	5.04
27	99	5.08	8.26	143	17.3	0.682	3.46

* Samples destroyed in transit

Table 14 - 1 - a

Fluxes of Particles by Size Fractions at 48°N 21°W, 1018 m and 1202 m; mg m^{-2} day^{-1}

Period	Mid JD	Total	>1mm	<1mm	>1mm (%)	<1mm (%)
1	96	48.8	5.28	43.5	10.8	89.2
2	105	81.9	5.05	76.9	6.17	93.8
3	119	102	1.53	101	1.49	98.5
4	133	140	4.56	136	3.25	96.8
5	148	159	12.9	146	8.08	91.9
6	164	82.6	7.59	75.0	9.19	90.8
7	178	26.7	2.11	24.6	7.91	92.1
8	192	41.8	5.23	36.6	12.5	87.5
9	206	44.1	18.7	25.4	42.4	57.6
10	220	59.7	15.4	44.4	25.7	74.3
11	234	37.4	5.57	31.8	14.9	85.1
12	248	29.8	1.53	28.3	5.12	94.9
13	262	69.9	9.72	60.2	13.9	86.1
14	279		— (Hiatus) —			
15	296	27.8	2.81	25.0	10.1	89.9
16	310	26.7	4.51	22.2	16.9	83.1
17	324	26.7	2.27	24.4	8.51	91.5
18	338	33.6	4.20	29.4	12.5	87.5
19	352	15.3	1.77	13.5	11.6	88.4
20	1	31.5	7.48	24.0	23.8	76.2
21	15	22.0	2.12	19.9	9.64	90.4
22	29	17.8	1.51	16.3	8.50	91.5
23	43	18.9	1.89	17.1	9.96	90.0
24	57	22.5	6.26	16.3	27.8	72.2
25	71	21.3	1.48	19.9	6.94	93.1
26	85	109	3.42	105	3.14	96.9
27	99	191	7.47	184	3.90	96.1

Table 14 - 1 - b

Fluxes of Ca, C_{inorg}, C_{org} and N_{org}
at 48°N 21°W, 1018 m and 1202 m

Period	Mid JD	$CaCO_3$	Ca in $CaCO_3$	C inorg	N org	C org	$CaCO_3$	Ca in $CaCO_3$	C inorg	N org	C org
		mg m^{-2} day^{-1}					percent				
1	96	23.5	9.40	2.82	0.698	4.57	48.1	19.3	5.77	1.43	8.82
2	105	41.6	16.7	4.99	0.614	6.75	50.8	20.3	6.10	0.750	4.71
3	119	63.2	25.3	7.59	0.953	8.53	61.7	24.7	7.40	0.930	5.49
4	133	87.2	34.9	10.5	1.14	9.76	62.2	24.9	7.46	0.810	4.66
5	148	90.7	36.3	10.9	1.54	15.5	57.0	22.8	6.84	0.970	5.54
6	164	55.4	22.2	6.65	0.933	8.06	67.1	26.9	8.05	1.13	7.15
7	178	14.4	5.77	1.73	0.504	5.57	54.0	21.6	6.48	1.89	12.5
8	192	17.3	6.93	2.08	0.702	8.90	41.4	16.6	4.97	1.68	13.7
9	206	19.3	7.75	2.32	0.904	11.3	43.9	17.6	5.27	2.05	14.9
10	220	25.6	10.3	3.08	0.842	13.4	42.9	17.2	5.15	1.41	11.7
11	234	17.6	7.04	2.11	0.595	8.65	47.0	18.8	5.64	1.59	13.1
12	248	17.2	6.87	2.06	0.382	4.82	57.5	23.0	6.90	1.28	10.9
13	262	39.8	15.9	4.78	0.866	10.3	57.0	22.8	6.84	1.24	10.7
14	279				— (Hiatus) —						
15	296	16.1	6.44	1.93	0.295	3.18	57.8	23.1	6.94	1.06	8.08
16	310	14.4	5.77	1.73	0.320	3.67	54.0	21.6	6.48	1.20	6.97
17	324	16.3	6.51	1.95	0.245	2.24	61.0	24.4	7.32	0.920	6.22
18	338	21.2	8.50	2.55	0.279	3.36	63.2	25.3	7.58	0.830	5.45
19	352	9.20	3.68	1.10	0.188	1.74	60.2	24.1	7.22	1.23	8.12
20	1	18.8	7.55	2.26	0.264	3.22	59.9	24.0	7.19	0.840	6.80
21	15	13.8	5.51	1.65	0.213	3.06	62.6	25.1	7.51	0.970	6.48
22	29	11.3	4.51	1.35	0.160	2.05	63.4	25.4	7.61	0.900	5.89
23	43	12.2	4.87	1.46	0.172	2.06	64.2	25.7	7.70	0.910	5.73
24	57	13.5	5.41	1.62	0.225	2.67	59.9	24.0	7.19	1.00	6.64
25	71	12.1	4.83	1.45	0.192	2.49	56.5	22.6	6.78	0.900	6.01
26	85	55.9	22.4	6.71	0.990	13.8	51.4	20.6	6.17	0.910	5.15
27	99	93.8	37.5	11.3	2.09	27.4	49.0	19.6	5.88	1.09	6.71

Table 14 - 1 - c

Opal Fluxes at 48°N 21°W, 1018 m and 1202 m

Period	Mid JD	SiO_2 opal	SiO_2 part	SiO_2 diss	Si in opal	SiO_2 opal	SiO_2 part	SiO_2 diss	Si in opal
		mg m^{-2} day^{-1}				percent			
1	96	13.6	11.2	2.40	6.34	27.8	22.9	4.91	13.0
2	105	18.1	16.5	1.67	8.47	22.1	20.1	2.03	10.3
3	119	19.0	17.2	1.73	8.85	18.5	16.8	1.69	8.63
4	133	28.0	26.2	1.80	13.1	20.0	18.7	1.28	9.33
5	148	40.0	38.5	1.52	18.7	25.2	24.2	0.953	11.7
6	164	8.03	6.60	1.43	3.75	9.73	8.00	1.73	4.54
7	178	3.41	2.56	0.850	1.59	12.8	9.60	3.19	5.97
8	192	6.82	5.69	1.13	3.18	16.3	13.6	2.71	7.62
9	206	5.82	5.07	0.755	2.72	13.2	11.5	1.71	6.17
10	220	8.29	7.47	0.820	3.87	13.9	12.5	1.37	6.48
11	234	5.18	4.60	0.576	2.42	13.8	12.3	1.54	6.46
12	248	4.05	3.73	0.315	1.89	13.6	12.5	1.06	6.33
13	262	9.43	8.94	0.481	4.40	13.5	12.8	0.689	6.30
14	279			— (Hiatus) —					
15	296	4.00	3.48	0.521	1.87	14.4	12.5	1.87	6.72
16	310	3.66	3.23	0.422	1.71	13.7	12.1	1.58	6.40
17	324	3.35	2.96	0.393	1.57	12.6	11.1	1.47	5.87
18	338	4.28	3.78	0.507	2.00	12.8	11.3	1.51	5.96
19	352	1.78	1.47	0.317	0.833	11.7	9.60	2.08	5.45
20	1	4.13	3.61	0.517	1.93	13.1	11.5	1.64	6.13
21	15	2.84	2.50	0.336	1.33	12.9	11.4	1.53	6.02
22	29	2.44	2.16	0.279	1.14	13.8	12.2	1.57	6.43
23	43	2.34	2.16	0.180	1.09	12.4	11.4	0.952	5.77
24	57	3.09	2.89	0.208	1.45	13.7	12.8	0.922	6.41
25	71	4.10	3.82	0.277	1.91	19.2	17.9	1.30	8.97
26	85	21.6	20.8	0.818	10.1	19.9	19.1	0.752	9.28
27	99	42.7	41.9	0.835	20.0	22.3	21.9	0.436	10.4

Table 14 - 1 - d

Phosphorus Fluxes at 48°N 21°W, 1018 m and 1202 m

Period	Mid JD	P total	P part	P diss	P total	P part	P diss
			$\mu g\ m^{-2}\ day^{-1}$			ppm	
1	96	656	0	656	1340	0	1340
2	105	1370	660	706	1670	806	862
3	119	1880	1138	742	1830	1110	723
4	133	2170	1220	952	1550	870	679
5	148	2050	1190	857	1290	748	539
6	164	652	0	652	789	0	789
7	178	673	354	319	2520	1330	1190
8	192	1070	483	584	2550	1160	1400
9	206	1190	582	608	2700	1320	1380
10	220	1420	733	691	2380	1230	1160
11	234	561	358	203	1500	956	543
12	248	638	247	391	2140	829	1310
13	262	1020	494	524	1460	706	750
14	279		— (Hiatus) —				
15	296	2200	300	1901	7910	1080	6830
16	310	1080	407	672	4040	1520	2520
17	324	928	241	687	3480	904	2580
18	338	679	289	390	2020	859	1160
19	352	1210	619	593	7930	4050	3880
20	1	659	322	337	2090	1020	1070
21	15	982	265	717	4460	1200	3260
22	29	253	137	116	1420	773	652
23	43	285	148	137	1510	784	722
24	57	491	203	288	2180	901	1280
25	71	325	181	144	1520	848	673
26	85	1610	1424	190	1480	1310	175
27	99	2910	1928	979	1520	1010	511

Table 14 - 1 - e

48°N 21°W, 1018 m and 1202 m
Ratios (Molar) of critical biogenic elements

Period	Mid JD	Ca/Si	C/N	C/P	N/P	C_{org}/C_{inorg}	C_{org}/Si
1	96	1.04	7.19	169	23.5	1.53	1.53
2	105	1.38	7.33	72.8	9.94	0.773	0.773
3	119	2.01	6.89	77.2	11.2	0.742	0.742
4	133	1.87	6.71	77.6	11.6	0.624	0.624
5	148	1.36	6.66	111	16.7	0.810	0.810
6	164	4.14	7.38	234	31.6	0.888	0.888
7	178	2.54	7.74	128	16.6	1.94	1.94
8	192	1.53	9.50	138	14.5	2.75	2.75
9	206	2.00	8.49	142	16.8	2.83	2.83
10	220	1.86	9.70	127	13.1	2.28	2.28
11	234	2.04	9.61	225	23.4	2.32	2.32
12	248	2.55	9.92	131	13.2	1.58	1.58
13	262	2.54	10.1	190	18.8	1.57	1.57
14	279		-- (Hiatus) —				
15	296	2.41	8.89	26.3	2.96	1.17	1.17
16	310	2.37	6.78	44.5	6.56	1.08	1.08
17	324	2.91	7.89	46.0	5.84	0.850	0.850
18	338	2.98	7.66	69.5	9.08	0.719	0.719
19	352	3.10	7.70	26.4	3.43	1.12	1.12
20	1	2.74	9.44	83.7	8.86	0.946	0.946
21	15	2.92	7.79	37.4	4.80	0.863	0.863
22	29	2.77	7.63	107	14.0	0.774	0.774
23	43	3.12	7.35	98.1	13.4	0.744	0.744
24	57	2.62	7.75	78.6	10.1	0.924	0.924
25	71	1.77	7.79	102	13.1	0.887	0.887
26	85	1.56	6.60	89.5	13.6	0.835	0.835
27	99	1.32	7.18	114	15.9	1.14	1.14

Table 14 - 2 - a

Fluxes of Particles by Size Fractions at 48°N 21°W, 2018 m and 2200 m; mg m^{-2} day^{-1}

Period	Mid JD	Total	>1mm	<1mm	>1mm (%)	<1mm (%)
1	96	36.4	0.00	36.4	0	100
2	105	74.0	1.77	72.3	2.40	97.6
3	119	82.6	2.92	79.7	3.53	96.5
4	133	101	1.48	99.1	1.47	98.5
5	148	247	4.09	242	1.66	98.3
6	164	153	2.22	151	1.45	98.6
7	178	204	1.89	202	0.926	99.1
8	192	59.9	0.45	59.5	0.749	99.3
9	206	86.2	1.68	84.5	1.95	98.0
10	220	68.0	1.35	66.6	1.98	98.0
11	234	76.6	8.20	68.4	10.7	89.3
12	248	74.8	3.75	71.0	5.02	95.0
13	262	98.7	41.7	56.9	42.3	57.7
14	279		— (Hiatus) —			
15	296	33.7	0.00	33.7	0	100
16	310	31.0	0.00	31.0	0	100
17	324	24.1	0.00	24.1	0	100
18	338					
19	352					
20	1					
21	15					
22	29					
23	43					
24	57					
25	71					
26	85					
27	99					

Table 14 - 2 - b

Fluxes of Ca, C_{inorg}, C_{org} and N_{org} at 48°N 21°W, 2018 m and 2200 m

Period	Mid JD	$CaCO_3$	Ca in $CaCO_3$	C inorg	N org	C org	$CaCO_3$	Ca in $CaCO_3$	C inorg	N org	C org
		mg m^{-2} day^{-1}					percent				
1	96	20.6	8.26	2.48	0.135	0.994	56.7	22.7	6.80	0.370	2.73
2	105	44.1	17.7	5.29	0.422	2.81	59.6	23.9	7.15	0.570	3.80
3	119	52.3	20.9	6.27	0.438	2.89	63.3	25.3	7.60	0.530	3.50
4	133	73.3	29.4	8.80	0.483	3.45	72.9	29.2	8.75	0.480	3.43
5	148	118	47.4	14.2	1.90	11.4	48.0	19.2	5.76	0.770	4.64
6	164	76.4	30.6	9.16	1.26	7.62	49.8	19.9	5.98	0.820	4.97
7	178	98.4	39.4	11.81	1.85	11.8	48.3	19.3	5.80	0.910	5.77
8	192	34.5	13.8	4.14	0.40	2.67	57.6	23.1	6.91	0.660	4.45
9	206	47.2	18.9	5.67	0.612	4.43	54.8	21.9	6.58	0.710	5.14
10	220	35.0	14.0	4.20	0.490	3.99	51.5	20.6	6.18	0.720	5.87
11	234	42.5	17.0	5.10	0.521	4.24	55.5	22.2	6.66	0.680	5.54
12	248	44.3	17.7	5.31	0.501	3.66	59.2	23.7	7.10	0.670	4.89
13	262	57.4	23.0	6.89	1.10	7.63	58.2	23.3	6.98	1.12	7.73
14	279				— (Hiatus) —						
15	296	20.3	8.12	2.43	0.230	1.59	60.2	24.1	7.22	0.680	4.71
16	310	18.7	7.49	2.24	0.210	1.55	60.4	24.2	7.25	0.680	5.00
17	324	13.7	5.47	1.64	0.290	1.94	56.7	22.7	6.80	1.19	8.05
18	338										
19	352										
20	1										
21	15										
22	29										
23	43										
24	57										
25	71										
26	85										
27	99										

Table 14 - 2 - c

Opal Fluxes at 48°N 21°W, 2018 m and 2200 m

Period	Mid JD	SiO_2 opal	SiO_2 part	SiO_2 diss	Si in opal	SiO_2 opal	SiO_2 part	SiO_2 diss	Si in opal
		mg m^{-2} day^{-1}				percent			
1	96	8.20	6.48	1.72	3.83	22.5	17.8	4.73	10.5
2	105	15.4	14.0	1.36	7.17	20.7	18.9	1.84	9.69
3	119	22.1	20.6	1.50	10.3	26.7	24.9	1.81	12.5
4	133	19.3	17.9	1.41	9.02	19.2	17.8	1.40	8.97
5	148	68.3	66.8	1.50	31.9	27.7	27.1	0.607	12.9
6	164	38.6	37.1	1.46	18.0	25.2	24.2	0.953	11.7
7	178	59.1	57.5	1.63	27.6	29.0	28.2	0.801	13.5
8	192	s	12.3	0.981	6.23	22.2	20.6	1.64	10.4
9	206	17.5	16.4	1.11	8.16	20.3	19.0	1.29	9.48
10	220	14.5	13.6	0.880	6.76	21.3	20.0	1.29	9.94
11	234	15.8	15.1	0.739	7.39	20.7	19.7	0.965	9.65
12	248	11.5	10.8	0.634	5.36	15.3	14.5	0.848	7.17
13	262	12.3	11.8	0.432	5.73	12.4	12.0	0.438	5.81
14	279			— (Hiatus) —					
15	296	5.82	5.08	0.740	2.72	17.3	15.1	2.20	8.07
16	310	4.85	4.45	0.480	2.26	15.7	14.4	1.29	7.31
17	324	3.39	2.96	0.430	1.58	14.1	12.3	1.78	6.57
18	338								
19	352								
20	1								
21	15								
22	29								
23	43								
24	57								
25	71								
26	85								
27	99								

Table 14 - 2 - d

Phosphorus Fluxes at 48°N 21°W, 2018 m and 2200 m

Period	Mid JD	P total	P part	P diss	P total	P part	P diss
		$\mu g\ m^{-2}\ day^{-1}$			ppm		
1	96	196	0	196	538	0	538
2	105	765	419	346	1030	566	468
3	119	916	544	372	1110	659	450
4	133	811	646	165	807	642	164
5	148	1810	1524	286	734	618	116
6	164	1630	1115	510	1060	727	333
7	178	1740	1257	483	854	617	237
8	192	421	306	115	702	511	191
9	206	977	498	479	1130	578	556
10	220	487	386	101	716	568	149
11	234	1100	938	165	1440	1220	216
12	248	629	494	135	841	661	181
13	262	2050	1524	524	2070	1540	531
14	279		— (Hiatus) —				
15	296	376	227	149	1110	674	443
16	310	371	216	154	1190	697	500
17	324	1340	655	687	5560	2720	2850
18	338						
19	352						
20	1						
21	15						
22	29						
23	43						
24	57						
25	71						
26	85						
27	99						

Table 14 - 2 - e

48°N 21°W, 2018 m and 2200 m
Ratios (Molar) of critical biogenic elements

Period	Mid JD	Ca/Si	C/N	C/P	N/P	C_{org}/C_{inorg}	C_{org}/Si
1	96	1.51	8.61	131	15.2	0.401	0.607
2	105	1.73	7.78	94.8	12.2	0.531	0.918
3	119	1.42	7.70	81.4	10.6	0.461	0.656
4	133	2.28	8.34	110	13.2	0.392	0.895
5	148	1.04	7.03	163	23.2	0.806	0.839
6	164	1.19	7.07	121	17.1	0.832	0.990
7	178	1.00	7.40	174	23.6	1.00	1.00
8	192	1.56	7.87	163	20.8	0.644	1.00
9	206	1.62	8.45	117	13.8	0.782	1.27
10	220	1.45	9.51	211	22.2	0.950	1.38
11	234	1.61	9.50	99.2	10.4	0.832	1.34
12	248	2.32	8.51	150	17.6	0.688	1.60
13	262	2.81	8.05	96.0	11.9	1.11	3.11
14	279		— (Hiatus) —				
15	296	2.09	8.08	109	13.5	0.652	0.137
16	310	2.32	8.58	108	12.6	0.690	1.60
17	324						
18	338						
19	352						
20	1						
21	15						
22	29						
23	43						
24	57						
25	71						
26	85						
27	99						

Table 14 - 3 - a

Fluxes of Size Fractions at 48°N 21°W, 3718 m and 3749 m; mg m^{-2} day^{-1}

Period	Mid JD	Total	>1mm	<1mm	>1mm (%)	<1mm (%)
1	96	37.1	0	37.1	0	100
2	105	55.0	0	55.0	0	100
3	119	74.9	3.91	71.0	5.22	94.8
4	133	72.6	1.80	70.8	2.47	97.5
5	148	164	2.85	162	1.73	98.3
6	164	200	1.59	198	0.80	99.2
7	178	187	2.07	185	1.11	98.9
8	192	142	4.96	137	3.48	96.5
9	206	113	0.988	112	0.88	99.1
10	220	95.4	0	95.4	0	100
11	234	55.8	0	55.8	0	100
12	248	71.3	0.853	70.4	1.20	98.8
13	262	85.7	41.7	44.0	48.7	51.3
14	279		— (Hiatus) —			
15	296	48.4	0	48.4	0	100
16	310	49.1	0	49.1	0	100
17	324	41.0	0	41.0	0	100
18	338	37.6	0	37.6	0	100
19	352	24.8	0	24.8	0	100
20	1	25.7	0	25.7	0	100
21	15	18.9	0	18.9	0	100
22	29	24.9	0	24.9	0	100
23	43	19.4	0	19.4	0	100
24	57	26.1	0	26.1	0	100
25	71	28.2	0	28.2	0	100
26	85	43.9	0	43.9	0	100
27	99	73.9	0	73.9	0	100

Table 14 - 3 - b

Fluxes of Ca, C_{inorg}, C_{org} and N_{org} at 48°N 21°W, 3718 m and 3749 m

Period	Mid JD	$CaCO_3$	Ca in $CaCO_3$	C inorg	N org	C org	$CaCO_3$	Ca in $CaCO_3$	C inorg	N org	C org
		mg m^{-2} day^{-1}					percent				
1	96	22.9	9.18	2.75	0.215	2.03	61.8	24.7	7.42	0.580	5.46
2	105	34.2	13.7	4.10	0.259	2.01	62.1	24.9	7.45	0.470	3.66
3	119	49.3	19.7	5.91	0.367	2.79	65.8	26.3	7.90	0.490	3.72
4	133	52.0	20.8	6.24	0.232	1.89	71.6	28.7	8.59	0.320	2.60
5	148	107	42.7	12.8	1.05	6.61	64.9	26.0	7.79	0.640	4.02
6	164	114	45.5	13.6	1.18	7.37	56.9	22.8	6.83	0.590	3.69
7	178	104	41.8	12.5	1.27	8.05	55.8	22.3	6.70	0.680	4.31
8	192	75.5	30.2	9.06	0.812	5.70	53.0	21.2	6.36	0.570	4.00
9	206	58.9	23.6	7.07	0.564	3.94	52.2	20.9	6.26	0.500	3.49
10	220	50.8	20.3	6.09	0.458	3.61	53.2	21.3	6.38	0.480	3.78
11	234	30.6	12.2	3.67	0.290	2.26	54.8	21.9	6.58	0.520	4.06
12	248	41.2	16.5	4.94	0.321	2.51	57.8	23.1	6.94	0.450	3.52
13	262	48.7	19.5	5.84	0.360	2.85	56.8	22.7	6.82	0.420	3.33
14	279				— (Hiatus) —						
15	296	29.5	11.7	3.51	0.26	2.09	60.5	24.2	7.26	0.530	4.33
16	310	25.2	10.1	3.02	0.25	1.78	51.3	20.5	6.16	0.500	3.63
17	324	24.7	9.91	2.97	0.21	1.65	60.4	24.2	7.25	0.510	4.02
18	338	23.9	9.57	2.87	0.17	1.37	63.5	25.4	7.62	0.450	3.63
19	352	14.9	5.97	1.79	0.13	1.04	60.0	24.0	7.20	0.520	4.18
20	1	16.2	6.48	1.94	0.13	1.02	63.0	25.2	7.56	0.500	3.95
21	15	11.1	4.46	1.34	0.10	0.08	58.9	23.6	7.07	0.550	4.21
22	29	16.1	6.43	1.93	0.12	0.90	64.5	25.8	7.74	0.470	3.61
23	43	11.8	4.73	1.42	.0.9	0.75	61.0	24.4	7.32	0.490	3.88
24	57	16.1	6.47	1.94	0.13	0.99	61.8	24.7	7.42	0.480	3.79
25	71	17.0	6.81	2.04	0.14	1.12	60.2	24.1	7.22	0.500	3.97
26	85	28.2	11.3	3.38	0.26	1.85	64.1	25.7	7.69	0.590	4.21
27	99	48.9	19.6	5.86	0.46	3.09	66.1	26.5	7.93	0.620	4.18

Table 14 - 3 - c

Opal Fluxes at 48°N 21°W, 3718 m and 3749 m

Period	Mid JD	SiO_2 opal	SiO_2 part	SiO_2 diss	Si in opal	SiO_2 opal	SiO_2 part	SiO_2 diss	Si in opal
		mg m^{-2} day^{-1}				percent			
1	96	7.18	6.05	1.13	3.35	19.4	16.3	3.06	9.04
2	105	10.7	9.74	1.02	5.03	19.6	17.7	1.86	9.13
3	119	10.8	9.51	1.27	5.04	14.4	12.7	1.70	6.72
4	133	8.75	7.69	1.06	4.09	12.1	10.6	1.46	5.63
5	148	39.2	37.9	1.31	18.3	23.9	23.1	0.80	11.1
6	164	52.0	50.4	1.60	24.3	26.0	25.2	0.80	12.1
7	178	45.6	44.1	1.53	21.3	24.4	23.6	0.82	11.4
8	192	35.8	34.5	1.30	16.7	25.1	24.2	0.91	11.7
9	206	30.1	29.1	1.02	14.1	26.7	25.8	0.91	12.5
10	220	23.2	22.2	0.906	10.8	24.3	23.3	0.95	11.3
11	234	12.4	11.7	0.609	5.75	22.1	21.0	1.09	10.3
12	248	16.4	15.8	0.605	7.64	23.0	22.1	0.85	10.7
13	262	17.1	16.7	0.299	7.94	19.9	19.5	0.35	9.27
14	279			— (Hiatus) —					
15	296	8.90	8.13	0.776	4.16	18.4	16.8	1.60	8.59
16	310	8.92	8.24	0.716	4.18	18.3	16.8	1.46	8.53
17	324	7.13	6.57	0.560	3.33	17.4	16.0	1.37	8.13
18	338	6.44	5.99	0.451	3.01	17.1	15.9	1.20	8.00
19	352	4.27	3.93	0.335	1.99	17.2	15.8	1.34	8.02
20	1	4.06	3.73	0.333	1.90	15.8	14.5	1.30	7.38
21	15	3.07	2.81	0.262	1.43	16.2	14.8	1.38	7.58
22	29	3.80	3.55	0.253	1.77	15.3	14.2	1.02	7.12
23	43	2.91	2.67	0.237	1.36	15.0	13.8	1.22	7.00
24	57	3.87	3.69	0.182	1.81	14.8	14.1	0.70	6.91
25	71	4.35	4.14	0.213	2.03	15.4	14.7	0.76	7.70
26	85	7.15	6.84	0.306	3.34	16.3	15.6	0.70	7.60
27	99	11.1	10.6	0.485	5.16	15.0	14.3	0.66	6.98

Table 14 - 3 - d

Phosphorus Fluxes at 48°N 21°W, 3718 m and 3749 m

Period	Mid JD	P total	P part	P diss	P total	P part	P diss
		$\mu g\ m^{-2}\ day^{-1}$			ppm		
1	96	444	0	444	1190	0	1190
2	105	363	263	100	659	477	182
3	119	543	370	173	725	494	231
4	133	329	264	64.8	452	363	89.3
5	148	944	859	84.7	573	522	51.5
6	164	1080	1008	71.6	540	504	35.8
7	178	891	808	83.8	477	432	44.9
8	192	797	672	124	559	472	87.5
9	206	530	480	49.8	469	426	44.1
10	220	442	397	44.4	462	416	46.5
11	234	295	255	40.4	529	457	72.4
12	248	328	298	29.5	459	418	41.3
13	262	26.8	0	26.8	31.2	0	31.2
14	279		— (Hiatus) —				
15	296	490	253	237	1010	524	489
16	310	490	410	79.3	999	837	161
17	324	283	231	51.8	691	565	126
18	338	220	181	38.6	584	482	102
19	352	289	174	114	1160	702	462
20	1	164	143	20.3	638	560	79.1
21	15	157	126	31.3	832	667	165
22	29	151	131	19.9	606	527	79.8
23	43	152	123	28.1	783	638	144
24	57	195	180	14.5	745	690	55.4
25	71	189	174	15.0	669	617	53.1
26	85	1010	385	622	2300	878	1420
27	99	1420	446	976	1920	604	1320

Table 14 - 3 - e

48°N 21°W, 3718 m and 3749 m
Ratios (Molar) of critical biogenic elements

Period	Mid JD	Ca/Si	C/N	C/P	N/P	C_{org}/C_{inorg}	C_{org}/Si
1	96	1.88	11.0	115	10.5	0.736	1.38
2	105	1.90	9.08	142	15.6	0.491	0.932
3	119	2.73	8.86	131	14.8	0.471	1.29
4	133	3.55	9.48	147	15.5	0.303	1.07
5	148	1.63	7.33	180	24.6	0.516	0.843
6	164	1.31	7.30	176	24.1	0.541	0.710
7	178	1.37	7.39	232	31.4	0.644	0.883
8	192	1.27	8.19	184	22.4	0.629	0.796
9	206	1.17	8.14	190	23.4	0.557	0.653
10	220	1.32	9.19	209	22.8	0.592	0.779
11	234	1.48	9.11	196	21.5	0.617	0.916
12	248	1.51	9.12	196	21.4	0.508	0.766
13	262	1.71	9.25	2479	268	0.489	0.837
14	279		— (Hiatus) —				
15	296	1.96	9.53	213	22.3	0.596	1.17
16	310	1.68	8.47	93.1	11.0	0.590	0.989
17	324	2.07	9.19	148	16.2	0.555	1.15
18	338	2.21	9.41	158	16.8	0.477	1.05
19	352	2.07	9.38	91.6	9.77	0.581	1.20
20	1	2.36	9.22	157	17.0	0.523	1.23
21	15	2.14	8.93	128	14.3	0.596	1.28
22	29	2.50	8.96	150	16.8	0.467	1.17
23	43	2.40	9.24	125	13.6	0.530	1.27
24	57	2.47	9.21	129	14.0	0.511	1.26
25	71	2.32	9.26	150	16.3	0.550	1.27
26	85	2.35	8.32	47.2	5.66	0.547	1.28
27	99	2.64	7.86	55.9	7.11	0.527	1.39

DOCUMENT LIBRARY

March 11, 1991

Distribution List for Technical Report Exchange

Attn: Stella Sanchez-Wade
Documents Section
Scripps Institution of Oceanography
Library, Mail Code C-075C
La Jolla, CA 92093

Hancock Library of Biology &
Oceanography
Alan Hancock Laboratory
University of Southern California
University Park
Los Angeles, CA 90089-0371

Gifts & Exchanges
Library
Bedford Institute of Oceanography
P.O. Box 1006
Dartmouth, NS, B2Y 4A2, CANADA

Office of the International
Ice Patrol
c/o Coast Guard R & D Center
Avery Point
Groton, CT 06340

NOAA/EDIS Miami Library Center
4301 Rickenbacker Causeway
Miami, FL 33149

Library
Skidaway Institute of Oceanography
P.O. Box 13687
Savannah, GA 31416

Institute of Geophysics
University of Hawaii
Library Room 252
2525 Correa Road
Honolulu, HI 96822

Marine Resources Information Center
Building E38-320
MIT
Cambridge, MA 02139

Library
Lamont-Doherty Geological
Observatory
Columbia University
Palisades, NY 10964

Library
Serials Department
Oregon State University
Corvallis, OR 97331

Pell Marine Science Library
University of Rhode Island
Narragansett Bay Campus
Narragansett, RI 02882

Working Collection
Texas A&M University
Dept. of Oceanography
College Station, TX 77843

Library
Virginia Institute of Marine Science
Gloucester Point, VA 23062

Fisheries-Oceanography Library
151 Oceanography Teaching Bldg.
University of Washington
Seattle, WA 98195

Library
R.S.M.A.S.
University of Miami
4600 Rickenbacker Causeway
Miami, FL 33149

Maury Oceanographic Library
Naval Oceanographic Office
Stennis Space Center
NSTL, MS 39522-5001

Marine Sciences Collection
Mayaguez Campus Library
University of Puerto Rico
Mayaguez, Puerto Rico 00708

Library
Institute of Oceanographic Sciences
Deacon Laboratory
Wormley, Godalming
Surrey GU8 5UB
UNITED KINGDOM

The Librarian
CSIRO Marine Laboratories
G.P.O. Box 1538
Hobart, Tasmania
AUSTRALIA 7001

Library
Proudman Oceanographic Laboratory
Bidston Observatory
Birkenhead
Merseyside L43 7 RA
UNITED KINGDOM

50272-101

REPORT DOCUMENTATION PAGE	1. REPORT NO. WHOI-92-15	2.	3. Recipient's Accession No.
4. Title and Subtitle Biogenic Particle Fluxes at the 34°N 21°W and 48°N 21°W Stations, 1989-1990: Methods and Analytical Data Compilation			5. Report Date March, 1992 6.
7. Author(s) Susumu Honjo and Steven J. Manganini			8. Performing Organization Rept. No. WHOI 92-15
9. Performing Organization Name and Address The Woods Hole Oceanographic Institution Woods Hole, Massachusetts 02543			10. Project/Task/Work Unit No. 11. Contract(C) or Grant(G) No. (C) OCE88-14228 (G)
12. Sponsoring Organization Name and Address Funding was provided by the National Science Foundation			13. Type of Report & Period Covered Technical Report 14.

15. Supplementary Notes

This report should be cited as: Woods Hole Oceanog. Inst. Tech. Rept., WHOI-92-15.

16. Abstract (Limit: 200 words)

This technical report represents the results of analyses on opal, organic carbon, nitrogen and phosphorus content in each of 156 specimen samples collected from the moored sediment trap experiment that was a part of JGOFS North Atlantic Bloom Experiment. The analyzed samples represent a spacio-temporal matrix formed by 6 time-series sediment traps that provided 26 periods of uniform and synchronized periods of 14 days. Traps were deployed at 3 depths, 1 km, 2 km and 0.7 km above the bottom, and at 2 stations, 34°N 21°W and 48°N 21°W from April 4, 1989 to April 17, 1990, as shown in Tables 1 and 2. Two of the periods were not 14 days, and there was an 18-day hiatus in September/October 1989 for changeover of the trap moorings. Some samples were unusable because of the intrusion of fish.

Samples were separated into several aliquots by wet-splitting, then water sieved into larger-than- and smaller-than-1-mm sizes. The fluxes of biogeochemical elements and constituents were determined on these aliquots and size fractions for: carbonate by vacuum gasometric method; opal by selective leaching method; reactive phosphorus by high temperature oxidation hydrolysis method; and organic carbon and nitrogen by applying an elementary analyzer. The annual fluxes, fluxes during the bloom, pre- and post-bloom episodes are summarized in Tables 4 to 9. Variability of particle fluxes by each period at the two stations in terms of size, fractions, sedimentary constituents and elements are shown in Tables 10 and 11. The Mol ratios between pairs of critical biogeochemical elements during each episode and annually, shown at various depths and stations, are included in Tables 7 through 11.

17. Document Analysis a. Descriptors

1. particle flux
2. bloom
3. North Atlantic Ocean
4. terminal ratio
5. ocean interior

b. Identifiers/Open-Ended Terms

c. COSATI Field/Group

18. Availability Statement	19. Security Class (This Report)	21. No. of Pages
Approved for publication; distribution unlimited.	UNCLASSIFIED	74
	20. Security Class (This Page)	22. Price